The Cryosphere, 20, 3271–3298, 2026
https://doi.org/10.5194/tc-20-3271-2026

The Cryosphere Open Access EGU

The influence of ocean waves on Antarctic sea-ice albedo and seasonal melting, and potential coupled physical and biological feedbacks

Robert A. Massom[1,2,3], Phillip A. Reid[4,2], Stephen G. Warren[5], Bonnie Light[5,6], Donald K. Perovich[7], Luke G. Bennetts[8,a], Petteri Uotila[9], Siobhan P. O'Farrell[10], Michael H. Meylan[11], Klaus M. Meiners[1,2,3], Pat Wongpan[1,2], Alexander D. Fraser[12,2], Alessandro Toffoli[13], Giulio Passerotti[13,14], Peter G. Strutton[12,3], Sean M. T. Chua[1,2], and Melissa Fedrigo[1]

[1]Australian Antarctic Division, Department of Climate Change, Energy, the Environment and Water, Kingston, Tasmania 7050, Australia
[2]Australian Antarctic Program Partnership, Institute for Marine and Antarctic Studies, Battery Point, Tasmania 7004, Australia
[3]ARC Australian Centre for Excellence in Antarctic Science, Institute for Marine and Antarctic Studies, Battery Point, Tasmania 7004, Australia
[4]Australian Bureau of Meteorology, Hobart, Tasmania 7000, Australia
[5]Department of Atmospheric and Climate Science, University of Washington, Seattle, Washington 98195, USA
[6]Polar Science Center, University of Washington, Seattle, Washington 98195, USA
[7]Thayer School of Engineering, Dartmouth College, Hanover, New Hampshire 03755, USA
[8]School of Mathematics and Statistics, University of Melbourne, Parkville, Victoria 3010, Australia
[9]Institute for Atmospheric and Earth System Research/Physics, Faculty of Science, University of Helsinki, 00170 Helsinki, Finland
[10]CSIRO Environment, Aspendale, Victoria 3195, Australia
[11]School of Computer and Information Sciences, University of Newcastle, Callaghan, New South Wales 2308, Australia
[12]Institute for Marine and Antarctic Studies, Battery Point, Tasmania 7004, Australia
[13]Department of Infrastructure Engineering, University of Melbourne, Parkville, Victoria 3010, Australia
[14]School of Computing and Information Systems, University of Melbourne, Parkville, Victoria 3010, Australia
[a]formerly at: School of Computer and Mathematical Sciences, University of Adelaide, Adelaide, South Australia 5005, Australia

Correspondence: Robert A. Massom (rob.massom@aad.gov.au)

Received: 2 July 2025 – Discussion started: 22 July 2025
Revised: 2 December 2025 – Accepted: 13 January 2026 – Published: 9 June 2026

Abstract. Identifying the full suite of processes that drive the melting of Antarctic sea ice each summer is crucial to improving the currently-poor ability of contemporary models to accurately simulate the climatological retreat phase of the annual sea-ice cycle. This is critical to (1) understanding and attributing observed trends and recent abrupt changes in sea-ice coverage and (2) the more robust prediction of future sea-ice conditions and impacts. This paper identifies wave-driven processes that can accelerate the seasonal melting of sea ice both in the marginal ice zone (MIZ) and in open-water areas within the interior sea-ice zone (SIZ). It builds on the long-held view that seasonal Antarctic sea-ice ablation is primarily driven by ice-floe lateral and basal melting enhanced in the MIZ by wave breakup of ice floes, by demonstrating that ocean waves play important additional roles in generating surface and interior melting (termed "*wave melting*") via three sets of processes: "*wave flooding*", "*wave pulverisation*", and "*wave greening*" (involving algal prolifera-

tion in wave-modified ice). Based on existing observations and simple one-dimensional modelling, these wave processes are estimated to reduce ice albedo by 0.38–0.64 compared to snow-covered ice, resulting in vertical melt-rate enhancements of 0.9–5.2 cm d^{-1} amplified by wave greening to 1.1–6.1 cm d^{-1}. The study also identifies five positive feedback and sub-feedback mechanisms that likely accelerate the ice melting further. It addresses a gap in current climate and Earth system models, which account for wave effects on floe-size distributions but overlook these coupled wave-driven dynamic, thermodynamic and biological processes that may contribute to explaining why and how Antarctic sea ice can melt back so rapidly each summer. An intention of this foundational study is to stimulate further targeted investigation aimed at quantifying the role of wave melting in the annual sea-ice cycle – as well as the contribution of wave greening to primary production in the sea-ice zone and its role in key biogeochemical processes that feed back to climate. The work has implications for planetary albedo, global climate feedbacks, marine ecosystems, and the accuracy of future sea-ice and climate projections in an increasingly-stormy Southern Ocean, as well as in a changing Arctic.

1 Introduction

1.1 Motivation and aims

Each year from late austral spring through summer, the Southern Ocean encircling Antarctica undergoes a remarkable large-scale transformation with the areal retreat of its sea-ice zone (SIZ) from ~ 18–20×10^6 km^2 in September to ~ 2–4×10^6 km^2 in February. The retreat largely occurs over just a 3-month period (November through January), whereas the autumn–winter advance phase lasts for 7 months (Comiso et al., 2017a). By comparison, the annual cycle of Arctic sea ice is approximately symmetrical (i.e., 6 months advance and 6 months retreat), reflecting the different geographical setting and processes occurring there (Parkinson, 2014; Maksym, 2019). To date, the rapid annual retreat of Antarctic sea ice has been largely attributed to lateral and basal – rather than surface and interior – melting of its constituent ice floes (Eayrs et al., 2019). The classical view is that this is driven by: (a) solar heating in leads (open-water gaps) between floes (Gordon, 1981) and within polynyas (Massom et al., 2003) that is related to the springtime increase of incident solar radiation (Roach et al., 2022); and (b) upwelling of relatively warm deep waters in certain regions (Gordon, 1981). Moreover, melting in the Antarctic marginal ice zone (MIZ) has been identified as making the largest contribution to the mean annual ice retreat across the entire Southern Ocean (Kimura et al., 2022), pointing to the need to better understand the climatological processes driving seasonal melting there. The Antarctic MIZ is the tens to hundreds of kilometres-wide region (Fraser et al., 2026) closest to the open ocean where the ice floes are influenced by ocean surface waves (Wadhams, 1986; Bennetts et al., 2024), which break up larger floes and prevent smaller floes from consolidating (Squire, 2007).

Here, and based on in situ observations, remote sensing and first-principle modelling calculations, we propose an additional factor that drives seasonal melting of Antarctic sea ice each late spring–summer and which will likely increase in importance in a predicted stormier Southern Ocean (Young et al., 2020), as well as becoming more prevalent in a changing Arctic. This is the role of ocean waves in decreasing the sea-ice albedo and in driving surface and interior melting, which we term "*wave melting*", by (1) flooding ice floes ("*wave flooding*") and (2) mechanically grinding down the ice and its snow cover into "*wave slush*" and brash ice ("*wave pulverisation*"). In addition, we propose that wave-flooding and wave-pulverisation processes create optimal habitat for enhanced ice algal production, and that the resultant darkening of the ice and wave ponds due to increased chlorophyll content (which we term "*wave greening*") further decreases the ice albedo, which increases the wave-melting rate. Moreover, we hypothesise that wave melting is additionally accelerated by three coupled positive feedbacks – which we term the "*wave-driven ice–albedo feedback*", the "*wave flooding–ice melting feedback*" and the "*wave flooding–floe fragmentation feedback*" – and that these are amplified by two biological-physical sub-feedbacks involving wave greening. We further propose that wave melting occurs not only in the MIZ but also within the interior SIZ when long-period swell penetrates deeply into the SIZ and adjacent to large open-water areas (leads and polynyas) with wind waves.

Where snow is present, it inhibits/delays sea-ice melt (Eicken et al., 1995) by virtue of its high albedo compared to bare sea ice (Perovich, 1996; Brandt et al., 2005; Zatko and Warren, 2015) and its low thermal conductivity (Sturm and Massom, 2017). The snow cover strongly reflects incoming solar radiation and decreases its absorption by, and transmission into and through, the underlying ice (Grenfell and Maykut, 1977; Grenfell and Perovich, 2004; Nicolaus et al., 2010). Moreover, snow buffers the ice below from air-temperature increases, including those associated with the frequent passage of storms, even in winter at the relatively-low latitudes attained by the MIZ (Massom et al., 1997).

The premise of this paper is that waves can dramatically alter the surface energy budget year round and drive surface melting of sea ice in summer – primarily by removing or substantially modifying the snow cover and/or pulverising the snow and ice to reduce the ice albedo, but also by directly exposing the ice surface to increased air temperatures and overwashing by warm seawater as summer progresses. The overall aims are (1) to show that previously-unconsidered wave-driven processes, feedbacks and effects could be significant – not only in the MIZ but also within the interior SIZ – and are therefore worthy of further investigation, and (2) to encourage and make recommendations for future research activities.

Specific aims are: (1) to make a preliminary estimate of the effect of waves on the daily vertical melt rate of a single localised ice floe (and/or area of wave-pulverised slush) as a function of latitude and time in the Antarctic SIZ in summer, by changing the ice albedo in the surface radiation energy budget; and (2) to introduce previously-unconsidered feedbacks that may accelerate wave melting. Regional to pan-Antarctic quantification of wave melting and associated feedbacks is not attempted in this study due to current lack of requisite observations, but is recommended as a high priority requiring targeted observations, analysis and modelling (see Sect. 6).

1.2 Context

To date, and in contrast to the Arctic (e.g., Tsamados et al., 2015), floe-surface and -interior melting as well as the possibility of associated ice–albedo and related feedbacks have been largely neglected as factors contributing to the rapid climatological seasonal melting of the Antarctic SIZ. This neglect is based on the dual premise that Antarctic sea ice largely retains its high-albedo and insulative snow cover into summer (Massom et al., 2001; Eayrs et al., 2019) while also lacking Arctic-like freshwater melt ponds (Andreas and Ackley, 1982; Drinkwater and Liu, 2000) that form from air-temperature-driven snow melt and pooling of the meltwater in surface depressions (Petrich et al., 2012). The general lack of surface melt ponds on Antarctic sea ice, apart from a few isolated observations (e.g. Takahashi, 1960; Corkill et al., 2023), has been attributed to the radiative and turbulent surface heat fluxes occurring there (Vihma et al., 2009). Complete synoptic-scale snow-melt episodes do occur at lower latitudes due to extreme air-temperature increases and even rainfall associated with the passage of storms, including in winter in the MIZ, but those events tend to be localised and short-lived (Massom et al., 1997).

Given these factors, the generally-used conceptual model for the broad climatological annual retreat of Antarctic sea ice is that each late-spring and summer, wind-driven Ekman divergence (Gordon and Taylor, 1975) associated with a twice-yearly deepening and poleward contraction of the circumpolar trough of sea-level pressure known as the Semi-Annual Oscillation (van Loon, 1967; Eayrs et al., 2019) pushes ice floes northwards into warmer waters where they melt. In addition, the ice divergence creates leads between floes that strongly absorb incoming solar radiation (Gordon, 1981; Enomoto and Ohmura, 1990; Nihashi and Ohshima, 2001). With the seasonal upturn in insolation following the September equinox (Roach et al., 2022), solar heating of the ocean's mixed layer then drives both lateral and basal melting of the floes (Maykut and Perovich, 1987). This further activates a positive "*ocean–ice albedo feedback*" (Nihashi and Cavalieri, 2006) related to the large difference in albedo between sea ice and open water, whereby solar heating in leads enhances lateral melt of floes and increases the open-water area, to enhance ice melt and so on in an amplifying cycle (Ebert and Curry, 1993; Curry et al., 1995; Ohshima and Nihashi, 2005; Kashiwase et al., 2017; Perovich and Richter-Menge, 2009).

Currently, ocean waves are largely considered to influence sea-ice melting only in terms of their important role in fracturing the MIZ ice cover into smaller floes (cf., Wadhams, 1986; Squire, 2007; Kohout et al., 2016). Small floes are more mobile and have a larger perimeter per unit area compared to larger floes (Maykut and Perovich, 1987; Toyota et al., 2006), leading to larger rates of lateral melting (Steele, 1992; Asplin et al., 2012, 2014; Perovich and Jones, 2014; Kohout et al., 2014) and basal melting (Horvat and Tziperman, 2018). Sea-ice and climate models now include the influence of waves on floe-size distributions (e.g., Bennetts et al., 2017; Roach et al., 2019; Bateson et al., 2020) – but not the role of waves in driving coupled flooding, snow removal, pulverisation and albedo reduction that lead to seasonal surface and interior melting of small wave-fragmented floes and wave-pulverised slush, as proposed here.

1.3 Significance

There is strong motivation to identify, understand and model the climatological processes and feedback mechanisms driving Antarctic sea-ice melt, including within the MIZ (Saiki et al., 2021). Such process knowledge is required (1) to rectify the current inability of contemporary models to accurately reproduce the rate and magnitude of the seasonal retreat phase observed in the satellite record since 1979 (cf., Eayrs et al., 2019; Roach et al., 2020), (2) to attribute observed Antarctic sea-ice trends and variability, and (3) to provide more-confident future projections (e.g., Notz and Bitz, 2017; Maksym, 2019; NAS, 2017; Roach et al., 2020). This priority need is underpinned by mounting concern over recent abrupt Antarctic sea-ice loss and its serious implications for the region and the Earth system (Kennicutt et al., 2014; Massom et al., 2018; Meredith et al., 2022; Abram et al., 2025). Since 2012, Antarctic sea-ice coverage has unexpectedly switched to a state of high variability (Turner and Comiso, 2017), with record high sea-ice extents in 2012–2014 (Reid and Massom, 2015) plummeting to record lows since 2016 – and with the biggest deficit occurring not only in the spring–summer melt period (Parkinson, 2019) but also in autumn–winter in 2023 through the present (Reid et al., 2024, 2025). There has also been a change to increased regional coherence in the pattern of sea-ice loss which is anomalous in the long-term record (Hobbs et al., 2024).

The unanticipated abruptness, magnitude and spatial coherence of this apparent regime shift raises concerns around potential acceleration of future Antarctic sea-ice loss in response to resultant changes in albedo and the surface energy budget (Riihelä et al., 2021) and activation and amplification of sea-ice-related albedo feedback mechanisms (cf., Goosse et al., 2018). At the same time, a change in the albedo of

the Antarctic SIZ (including the ice itself) has the potential to amplify high-latitude climate warming in the Southern Hemisphere, as it has in the Arctic (Manabe and Stouffer, 1980; Meehl and Washington, 1990; Holland and Bitz, 2003; Screen and Simmonds, 2010). Model analyses by Goosse et al. (2023) highlight the key importance of albedo in the annual Antarctic sea-ice cycle and as a prime target for process understanding and model development. Here, we provide mechanisms that modify the surface albedo, as well as the thickness distributions and volume of the sea ice and its snow cover – all of which are major unknowns in the global climate system which severely compromise modelling performance and predictive capability (Maksym et al., 2012; Webster et al., 2018).

2 Data and techniques

2.1 Observations

Wave-melting phenomena and processes are identified here based on shipborne observations and photographs acquired from multiple voyages across the Antarctic SIZ, particularly the MIZ, and from the literature (e.g., Ackley, 1985; Massom, 1991; Ackley and Sullivan, 1994; Massom et al., 1997, 1998, 1999, 2001, 2006). As no direct measurements are available for albedos of wave-flooded and wave-pulverised ice, we use proxy estimates of albedos for the different wave-affected surface types derived from measurements made from ships and helicopters, as described in Sect. 3.2 below. Daily sea-ice concentrations for calculating the distance to the ice edge (Sect. 3.1.2) and the latitude of ice within the MIZ (Sect. 3.3) are based on daily satellite passive-microwave ice-concentration data dating back to 1979 (Cavalieri et al., 1996, updated yearly). The sea-ice edge is delineated by the 15 % ice-concentration isoline.

2.2 Computing radiative transfer and wave-driven melt-rate enhancement

Here, we consider the effect of wave flooding and wave pulverisation on only the shortwave properties of an ice floe/area of wave slush, which is to reduce the sea-ice albedo. The longwave (infrared) emissivities of snow, ice and water are all close to 100 % (Warren, 1982, 2019), so the only longwave effect of wave flooding is to increase the longwave emission slightly by increasing the surface temperature of the ice, bringing it up to $\sim 0\,^{\circ}\mathrm{C}$.

Our computation starts with the daily-average incident solar flux at the top of the atmosphere, F_{TOA} (in $\mathrm{W\,m^{-2}}$), and then multiplies it by the atmospheric transmittance over Antarctic sea ice, τ_{a}, to obtain the solar flux at the surface (F_{sfc}, in $\mathrm{W\,m^{-2}}$) as

$$F_{\mathrm{sfc}} = \tau_{\mathrm{a}}\, F_{\mathrm{TOA}} \tag{1}$$

Following Fitzpatrick and Warren (2005; FW05), and as τ_{a} is not directly available, we take two steps to obtain F_{sfc}. We first obtain the transmittance, τ_{clr}, for clear sky (shown in Fig. 7 of FW05 as a linear fit versus solar zenith angle θ), such that

$$\tau_{\mathrm{clr}} = 1.03 - 0.0046\,\theta \tag{2}$$

with θ in degrees. Then we apply the "cloud radiative forcing" CRF as a correction, to obtain F_{sfc} as

$$F_{\mathrm{sfc}} = \tau_{\mathrm{clr}}\, F_{\mathrm{TOA}} + \mathrm{CRF_d} \tag{3}$$

where $\mathrm{CRF_d}$ is the downward shortwave cloud radiative forcing in $\mathrm{W\,m^{-2}}$ (measured by FW05 and plotted in their Fig. 10), which is a negative quantity, indicating that clouds reduce the downward solar flux at the surface.

We estimate the albedo change (decrease), $\Delta\alpha$, caused by wave flooding of a snow-covered floe of wave pulverisation to be

$$\Delta\alpha = \alpha_{\mathrm{s}} - \alpha_{\mathrm{w}} \tag{4}$$

where α_{s} is the albedo of a snow-covered floe of first-year ice (FYI), and α_{w} is the albedo of wave-flooded and/or wave-pulverised ice. Multiplying F_{sfc} by $\Delta\alpha$ gives the radiative forcing, $\mathrm{RF_w}$, of wave-flooded or wave-pulverised ice as

$$\mathrm{RF_w} = \Delta\alpha\, F_{\mathrm{sfc}} \tag{5}$$

which is in units of $\mathrm{W\,m^{-2}}$. Equation (5) holds for a single idealised sea-ice slab or small area of (unconsolidated) wave slush at a given latitude and day of year. Due to current lack of important spatio-temporal information, e.g., on the extent and fractional coverages of the different wave-flooded types and wave-pulverised ice, it is beyond the scope of this study to estimate regional averages of radiative forcing ($\mathrm{RF_{w,avg}}$) as a function of latitude, longitude and month. Our aim is simply to show that wave flooding, wave pulverisation and wave greening likely enhance seasonal sea-ice melting, and are worthy of further investigation and modeling.

To estimate the change in melt rate of the idealised wave-flooded small floe and/or area of wave slush due to the radiative forcing, i.e., the wave-driven *melt-rate enhancement*, we divide the radiative forcing (Eq. 5) by the sea-ice density, $\rho = 905\,\mathrm{kg\,m^{-3}}$ (Fang et al., 2022), and the latent heat of fusion, $L = 334\,\mathrm{J\,g^{-1}}$ (Fang et al., 2022), to obtain

$$\frac{\mathrm{d}h}{\mathrm{d}t} = \frac{\mathrm{RF_w}}{(\rho\, L)} \tag{6}$$

where h is the sea-ice thickness and t is time.

3 Results

3.1 Wave melting processes

We identify the following wave-driven processes that contribute to seasonal wave melting, with closed circles denot-

ing main processes, open circles sub-processes and dashes sub-sub-processes:

- Wave Flooding (physical seawater-inundation processes)
  - Wave overwashing
  - Wave ponding
    - Wave-buffeting ponding
    - Wave-deformation ponding
  - Wave-compression flooding
- Wave Pulverisation (mechanical grinding down of floes into wave slush and brash ice)
  - Wave churning
- Wave Greening (algal proliferation and ice/wave-pond darkening)

Example images are shown in Fig. 1, with schematic representations of wave fracturing, wave flooding, wave pulverisation and wave greening in Fig. 2. The images in Fig. 1a–f and h are oblique views taken from the Australian icebreaker *RSV Aurora Australis* during experiments in the East Antarctic sector in late austral winter to early spring, while the wave-pulverisation and wave-slush images (Fig. 1i, j) were acquired from the US icebreaker *RSV Nathaniel B Palmer* in the Bellingshausen Sea during the late austral spring. Figure 1g is a larger vertical view of wave-compression flooding from an aerial camera on a helicopter of the scene shown in Fig. 1h.

Wave-flooding processes are not to be confused with flooding due to floe-surface submergence under the weight of overlying snow (Wadhams et al., 1987; Massom et al., 2001). This latter style of flooding is widespread across the Antarctic SIZ (Eicken et al., 1994; Maksym and Markus, 2008), but it seldom results in complete snow removal and exposed ponding because only the lowest part of the snowpack is typically flooded (Massom et al., 2001).

3.1.1 Wave overwashing

Wave overwashing is widespread in the outer MIZs in both the Antarctic (Massom et al., 1997, 1998) and the Arctic (Massom, 1991), where it typically affects small floes (<5 m diameter) that are themselves the product of wave-driven fracturing of larger floes. Floes smaller than or comparable to the prevailing wavelengths tilt with the incoming waves but slightly out-of-phase with them, such that overwashing is generated at the leading and trailing floe edges as they pitch below the ocean surface (Skene et al., 2015; Toffoli et al., 2015; Nelli et al., 2020). This causes seawater to flow (wash) back and forth across their surfaces (e.g., floes marked OWF in Figs. 1a and b; and 2b and c), where it can either push the snow cover into the ocean and/or turn it into a slush layer on the floe surface. In contrast, floes larger than the prevailing wavelengths, and directly exposed to open water, are overwashed by waves breaking over their leading edge and onto the floe surface (Passerotti et al., 2022; Fig. 2c). Wave overwashing can also thrust sea-ice blocks onto the surfaces (margins) of small floes, to weigh down that part of the floe, decrease its freeboard and increase the likelihood of further overwashing and flooding (see Sect. 3.1.2 below).

Wave overwashing is not restricted to the MIZ; it also affects floes adjacent to large open-water areas, i.e., leads and polynyas, as observed for example in the Weddell Sea (Massom et al., 1997) and the East Antarctic sector (Massom et al., 1998). This is due to the prevalence of wind waves there, generated by katabatic winds in coastal regions, e.g., within polynyas (cf., Ackley et al., 2020; Herman and Bradtke, 2024) and the frequent passage of storms across the wider SIZ (cf., Godfred-Spenning and Simmonds, 1996; Uotila et al., 2011). For example, Ackley et al. (2020) observed significant-wave heights in excess of 2 m in the Terra Nova Bay Polynya (Ross Sea) in May. Large leads are a prevalent feature within the Antarctic SIZ (Dubey et al., 2025) due to its largely-divergent nature with the frequent passage of storms (Worby et al., 1998), with lead widths of up to 6500 m observed in the Weddell Sea by Muchow et al. (2021), while recurrent and persistent coastal polynyas are widely distributed around Antarctica along with fewer open-ocean polynyas (Barber and Massom, 2007).

3.1.2 Wave ponding

We further propose that the ponding of seawater on ice-floe surfaces can occur by a set of ice-deformation processes driven not only by winds and currents but also by ocean waves ("*wave ponding*"). By one sub-process that we term "*wave buffeting*", the constant collision, jostling and rotation of small floes (typically <5 m across) driven by incoming waves rounds off their angular edges and creates decimetre-scale raised rims (e.g., floe marked WBP in Figs. 1c; 2d). Where these rims form around the entire floe perimeter (which is often the case), they act as mini ice levées that entrap and retain seawater introduced onto the surface by wave overwashing (Fig. 2d) and/or via the upward movement of seawater through the ice if it is permeable (cf., Golden et al., 1998) and has a negative freeboard. We term this sub-class of saline wave ponds *wave-buffeting ponds*. Such ponds can be maintained by constant wave overwashing, but they can also freeze and accumulate a snow cover in the cold season and where wave energy dies down.

In the typical example shown in Fig. 1c, wave-buffeting ponding is visually estimated to cover about one third of surface area of the small floes, which comprise about 65 % of the image scene (the remaining 35 % being a mix of open water and wave slush – see Sect. 3.1.4 for discussion of wave slush). This example, from 11 October 2007 at ∼ 62.5° S and 123.7° E, is about 25 km south of the ice edge as demarcated by the 15 % sea-ice concentration isoline. Another example in Fig. 1d shows extensive coverage of wave-buffeting pond-

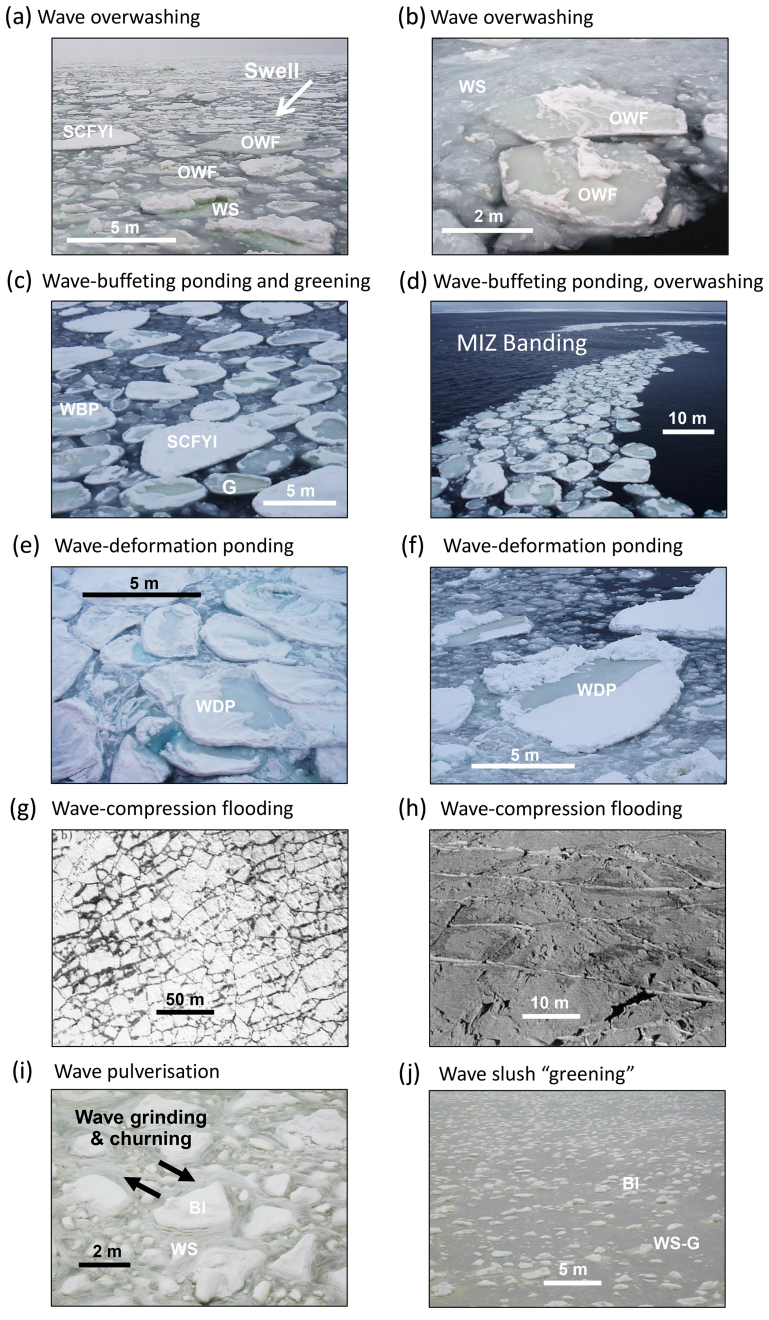

Figure 1. Photographic examples of wave flooding, wave pulverisation and wave greening, with estimates of ice thickness (h) and sea-ice surface water (wave pond) depth (h_w) from the ship: **(a–b)** wave overwashing ($h \sim 100$ cm, $h_w \sim 1$–5 cm); **(c)** wave-buffeting ponding and wave greening ($h \sim 70$ cm, $h_w \sim 5$ cm); **(d)** marginal ice zone (MIZ) banding with wave-buffeting ponding and wave overwashing ($h \sim 50$–70 cm, $h_w \sim 5$ cm); **(e–f)** wave-deformation ponding ($h \sim 70$–100 cm, $h_w \sim 5$–20 cm); **(g–h)** wave-compression flooding from aerial photography and from the surface, respectively ($h \sim 70$ cm); **(i)** wave pulverisation (wave-slush thickness ~ 50–100 cm), with black arrows denoting wave grinding and wave churning; and **(j)** wave-slush greening (wave-slush thickness ~ 50–100 cm). OWF indicates wave-overwashed floe; SCFYI is snow-covered first-year ice; WS is wave slush; WBP is wave-buffeting pond; WDP is wave-deformation pond; G is greening; and BI is brash ice.

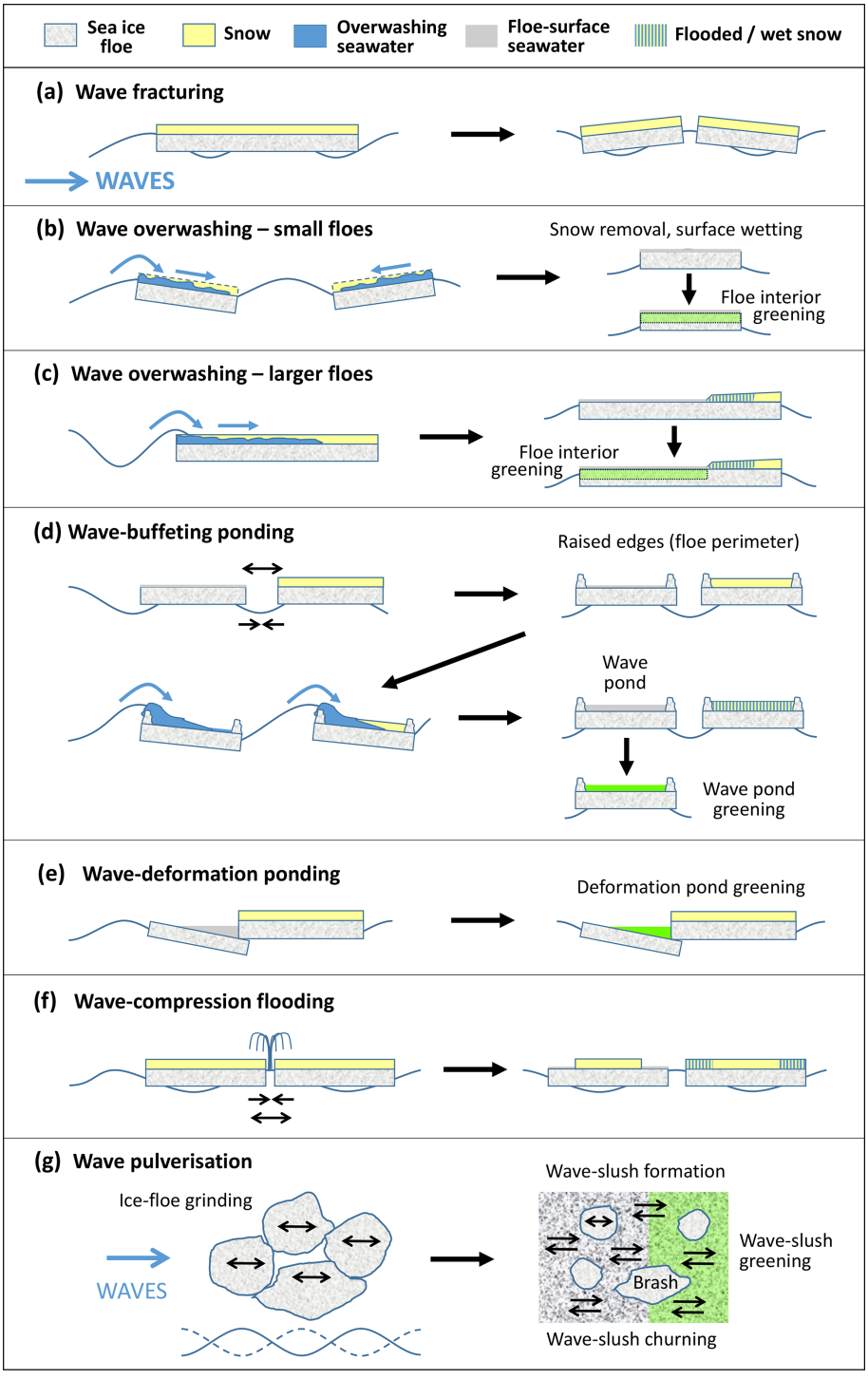

Figure 2. Schematic representation of **(a)** wave fracturing; **(b–c)** wave overwashing for large and small floes, respectively, and greening; **(d)** wave-buffeting ponding and greening; **(e)** wave-deformation ponding and greening; **(f)** wave-compression flooding; **(g)** wave pulverisation with wave churning leading to wave-slush formation, and wave-slush greening. Representative images of **(b)**–**(g)** are shown in Fig. 1.

ing in an ice-edge band, fields of which are a ubiquitous feature of the MIZ (cf., Ishida and Ohshima, 2009). They may extend the spatial and temporal influence of wave melting; this is covered in Sect. 4.2.

Surface seawater inundation and snow removal can also occur where incoming waves drive convergence and deformation in the sea-ice field and push floe surfaces below sea level, leading to "*wave-deformation ponding"* where there is connection to the underlying ocean (cf., Massom et al., 1997, 1998). This second sub-process of wave ponding can occur where waves drive the over-rafting of small floes and/or the mechanical pile-up of ice rubble on their surfaces (cf., Dai et al., 2004; Bennetts and Williams, 2015; Sutherland and Dumont, 2018); an example is given in Fig. 1e, with a schematic depiction in Fig. 2e. Wave-deformation ponding can also occur where wave-driven fracturing of a floe adjacent to an existing pressure ridge can place the surface of the resultant smaller floe out of isostatic balance due to the weight of the ridged ice (that was originally spread over a larger floe) – leading to partial submergence, seawater flooding and ponding as the new floe readjusts (cf., Ackley, 1985; Ackley and Sullivan, 1994). An example is shown in Fig. 1f. Flooded areas caused by pressure-ridge loading have been termed surface-saline ponds by Ackley and Sullivan (1994), but we retain the term wave-deformation ponds here as surface-saline ponds can also occur in the interior SIZ due to sea-ice convergence and deformation driven by winds and ocean currents. Deformation-type ponds have been observed to cover ∼ 5 %–10 % of the total surface area of the sea-ice floes about 200 km poleward of the ice edge and in winter, in the northwestern Weddell Sea (Massom et al., 1997), the western Weddell Sea (Ackley and Sullivan, 1994) and the western Pacific Ocean sector (Massom et al., 1998).

Henceforth and for the purposes of investigating their impact on ice albedo and wave melting, wave-buffeting ponds and wave-deformation ponds are collectively referred to as "*wave ponds*". Although wave ponds in some ways resemble seasonal Arctic melt ponds, they are saline rather than freshwater (low salinity) and occur year-round, i.e., they are not confined to the summer melt season and form faster than Arctic melt ponds (cf., Lüthje et al., 2006; Webster et al., 2022).

3.1.3 Wave-compression flooding

Under certain circumstances, long-period swells penetrate hundreds of kms into the Antarctic SIZ from the ice edge (Liu and Mollo-Christensen, 1988; Nose et al., 2023; Morris et al., 1998; Worby et al., 1998; Kohout et al., 2014). In addition to potentially driving wave-deformation ponding, deep swell penetration can lead to "*wave-compression flooding*" in extensive areas of consolidated and undeformed FYI (Massom et al., 1999). By this process (Fig. 2f) and in the example given in Fig. 1g–h from the East Antarctic SIZ in August 1995, incoming swells caused linear lateral and transverse through-cutting breaks (cracks) in large FYI floes of uniform thickness (estimated ∼ 0.7 m). These cracks opened and then closed a few seconds later with the passage of each wave crest and trough, leading to compression of seawater between the two converging ice plates (Massom et al., 1999). This resulted in the "squirting" of seawater onto the surface of the newly-created, small angular floes around their perimeter (Worby et al., 1998). Analysis of aerial photographs along the 139°15′ E meridian revealed that this wave-compression flooding event affected a zonal band ∼ 70 km wide and up to 360 km south of the ice edge (Massom et al., 1999). This process wetted and darkened an estimated 20 % of the surface of 100 %-concentration sea ice (seen as a greying of the snow cover adjacent to the cracks, determined from the aerial photos). The frequency of occurrence of such wave-compression flooding events is unknown.

3.1.4 Wave pulverisation

While there has been emphasis on the role of waves in the flexural breakup of larger floes into smaller floes in the MIZ (e.g., Kohout et al., 2014), we here highlight an additional wave-driven process in floe breakdown and melting. This is the lateral grinding together and mechanical pulverisation of small floes by incoming swells (Fig. 2g), resulting in an agglomeration of (1) small brash-ice fragments that are easily flooded by waves and (2) an unconsolidated slushy mix of pulverised ice and snow (Massom et al., 2006) that we term "*wave slush*". In the colder months, this wave slush is likely supplemented by, and potentially enhances, frazil-ice formation. Wave pulverisation is distinct from the flexural fracturing of floes by waves, which decreases their size as depicted in Fig. 2a (cf., Squire, 2007), and we propose here that it contributes to a wider reduction in surface albedo and an increase in melt rate (compared to snow-covered floes).

In an October 2001 observation from the Bellingshausen Sea (Fig. 1i), persistent northwesterly winds compacted the SIZ against the western Antarctic Peninsula, while a 2–3 m northwesterly swell mechanically pulverised the ice cover within the highly-compact MIZ over a distance of tens of kilometres in from a linear ice edge (Massom et al., 2006). This created a continuous (100 % cover) agglomeration of brash ice fragments ($< \sim 1$ m across) and unconsolidated wave slush which was constantly reworked by the incoming swells, by a sub-process that we term "*wave churning*". Interstitial wave slush and brash ice also occur between larger contiguous floes in such wave-affected areas e.g., Fig. 1a–b and f.

3.1.5 Wave greening

We propose that wave flooding and wave pulverisation and associated snow removal create an ideal habitat for proliferation of ice algae within wave ponds (e.g., floe marked G in Fig. 1c) and/or in the snow-free ice column (particularly in

late spring–summer) – and that this wave greening (darkening due to high chlorophyll and other algal pigment content) further reduces the ice albedo (see Sect. 3.2 and 3.3). Light attenuation by snow is a major limiter of ice-algal growth (Arrigo et al., 2014), and snow-cover removal by waves increases the exposure of low-light-adapted algae to substantially higher levels of photosynthetically-active radiation to potentially enhance primary production within the wave-flooded ice. Wave flooding likely also introduces biogenic material and nutrients onto floe surfaces, where they are retained in wave ponds and/or continually replenished by wave overwashing. While no direct measurements of wave-pond habitats are yet available, limited observations have shown similar surface-saline ponds to support high algal biomass (chlorophyll content) and act as mini oases of high primary production within ice-covered areas (Kottmeier and Sullivan, 1990; Ackley and Sullivan, 1994; Garrison et al., 2003; Arrigo et al., 2014). This greening and darkening of wave ponds contrasts with Arctic freshwater meltponds, which generally contain low algal biomass due to low nutrient concentrations (Arrigo et al., 2014).

In the case of wave pulverisation, and in the example from the Bellingshausen Sea MIZ in October 2001 shown in Fig. 1j, the mechanical grinding together of floes and resultant release of ice algae created an extensive area of unconsolidated green wave slush and brash-ice fragments <1 m across, that was constantly churned and mixed by the incoming swells (Fig. 2g). This exposed the ice algae to significantly higher light and nutrient levels than in a snow-covered floe, leading to an intense "intra-ice algal bloom", i.e., unusually early in the sunlit season and relatively far south at $\sim 65^\circ$ S and also undetectable in satellite ocean-colour data (Massom et al., 2006).

3.2 Wave modification of sea-ice albedo

To our knowledge, spectral albedo has not yet been directly measured for wave-flooded and wave-pulverised ice (and their wave-greened equivalents). For this initial study, we therefore use surrogate estimates of spectral albedo based on measurements from ships and helicopters for types of Antarctic sea ice, both bare and snow-covered, that we consider to have similar albedos to the wave-affected ice types. Brandt et al. (2005) and Zatko and Warren (2015) summarise the measured albedo values, where spectral values are integrated over wavelength (weighted by the solar spectral flux) to obtain band-average albedos for narrow- and broad-bands, and for both clear and cloudy skies. Here we use averages over the entire solar spectrum (290–3000 nm wavelengths), which we call "broadband albedo" (Table 1). We list the albedos for cloudy sky rather than clear sky, as they are the most relevant to the Antarctic SIZ given that average cloud coverage there exceeds 80 % in spring–summer (Warren et al., 1988; Fitzpatrick and Warren, 2007). Immediately apparent is the strong sensitivity of sea-ice albedo to even a thin layer of snow, with snow-free FYI floes having average broadband albedos which are 0.3 less than their snow-covered counterparts (Table 1). Therefore, snow removal (e.g., by waves) is of crucial importance in terms of its effect on the radiation energy budget and the seasonal melt rate of sea ice.

Albedo has not been measured for wave-flooded or wave-pulverised ice floes, excepting Allison et al. (1993) who reported an albedo of 0.68 for a mixture of pancake ice, nilas and brash ice. However, that albedo value depends on the relative amounts of the three ice types present, so we do not use it in our calculations. Instead, we use Zatko and Warren (2015)'s measured albedo for four cases of slush formed by snow blowing into a lead in the Antarctic SIZ, as a surrogate for wave slush formed by wave pulverisation processes (Fig. 1i), wave compression-flooded ice (Fig. 1g, h) and wave-overwashed FYI (Fig. 1a, b), based on their similar appearance.

To represent wave ponds, we use albedos measured on Arctic melt ponds with similar appearance (Light et al., 2022). Most Arctic melt ponds are darker than Antarctic wave ponds, because melt ponds overlay waterlogged ice (the snow is long-gone) whereas wave ponds are typically brighter as they consist of slush or water over relatively bright ice. However, many Arctic melt ponds do resemble the wave ponds shown in Fig. 1c–f, and those melt ponds are the ones we use as surrogates. The surrogate broadband albedo values for the different wave-affected surface types are given in Table 2. Table 2 also includes surrogate albedo estimates for wave-ponded, bare and wave-pulverised ice types modified by wave greening. In the absence of direct measurements and for the purpose of this initial study, the greening is estimated (assumed) to darken the ice, reducing the albedos of these types by an additional 0.1 compared to their "non-green" counterparts.

We compare these surrogate average broadband albedo values with that observed for non-wave-greened thick FYI with a snow cover ($\alpha = 0.84$) to determine the decrease in average broadband albedo ($\Delta\alpha$) for the four different wave-affected albedo-type classes A–D given in Table 2. Thick FYI with a snow cover is chosen as the reference/baseline for this initial study as it has the highest albedo (Table 1). Estimated values of $\Delta\alpha$ given in Table 2 range from 0.38 to 0.64.

These values of $\Delta\alpha$ form the basis for our first approximation of the resultant increases in the daily vertical melt rates of the wave-affected surface-type classes in the Antarctic SIZ in summer due to wave melting, compared to a snow-covered FYI floe (Sect. 3.3 below). More detailed analysis of the influence of wave melting on larger regional to pan-Antarctic scales, and as a function of time of year, is not attempted due to current lack of key large-scale information on the spatio-temporal coverage of wave flooding and wave pulverisation – but is recommended as priority future work when observations become available (see Sect. 6).

Table 1. Broadband albedos for open water, bare ice, snow-covered ice and snow slush measured in the Antarctic SSIZ, under a cloudy sky (Brandt et al., 2005; Zatko and Warren, 2015) and used as the basis of surrogate estimates of broadband albedos of the different wave-flooded and wave-pulverised types in Table 2.

Surface type	Albedo range	Average albedo
Open water	0.06–0.07	0.07
First-year ice (<0.7 m), bare	0.41–0.49	0.45
First-year ice (<0.7 m) with 2–4 cm snow	0.70–0.78	0.74
First-year ice (>0.7 m), bare	0.50–0.58	0.54
First-year ice (>0.7 m) with >3 cm snow	0.82–0.87	0.84
Wave-pulverised ice plus pancake ice, one case only (Allison et al., 1993, their Fig. 12)	0.68	–
Snow slush (average and range of 4 cases)	0.35–0.59	0.46

Table 2. Surrogate estimates of broadband albedos under a cloudy sky for the four broad albedo classes of wave-affected sea ice: (A) wave-overwashed FYI, wave-compression flooded ice and wave slush; (B) wave slush darkened by wave greening; (C) wave ponds; and (D) wave ponds and/or *wave-overwashed ice with no snow cover.

Wave-affected surface type	α class	Photos in Fig. 1	Albedo range	Average albedo	$\Delta\alpha$
Overwashed first-year ice Wave-compression flooded Wave slush	A	a, b g, h i	0.35–0.59	0.46	0.38
Wave slush – green	B	j	0.25–0.49	0.36	0.48
Wave-buffeting pond Wave-deformation pond	C	c, d e, f	0.2–0.4	0.3	0.54
Wave pond, bare ice* – green	D	c	0.1–0.3	0.2	0.64

3.3 Wave enhancement of sea-ice vertical melt rate

We first compute the wave-driven enhancement in vertical melt rate ($\mathrm{d}h/\mathrm{d}t$) based on the radiative effects of both wave flooding and wave pulverisation on the December solstice (the approximate midpoint of the austral-summer melt season) and for single parcels of ice at 65° S (a representative latitude of the MIZ e.g., for much of East Antarctica and the Ross Sea at that time of year [Massom et al., 2013]). In order to illustrate the technique and the magnitude of the effect, we initially focus on Type A (wave-overwashed ice, wave compression-flooded FYI and wave slush), where $\Delta\alpha = 0.38$ (Table 2).

On the December solstice at 65° S, the downward shortwave (SW) flux at the top of the atmosphere (F_{TOA}) is 510 $\mathrm{W\,m^{-2}}$ (Fig. 2.7 of Hartmann, 2016). This corresponds to an effective daily-average solar zenith angle of 68° (solar constant is 1360 $\mathrm{W\,m^{-2}}$; $\cos^{-1}(510/1360) = 68°$). For solar zenith angle 68°, we get the downward SW at the surface, F_{sfc}, as described in Sect. 2.2. The corresponding atmospheric transmittance over sea ice is $\tau_{\mathrm{a}} = 0.52$, so $F_{\mathrm{sfc}} = 0.52 \times 510 = 264\,\mathrm{W\,m^{-2}}$. Referring back to Eq. (5), the radiative forcing caused by wave flooding ($\mathrm{RF_w}$) is:

$$\mathrm{RF_w} = \Delta\alpha\, F_{\mathrm{sfc}} = 0.38 \times 264 = \sim 100\,\mathrm{W\,m^{-2}}.$$

For an idealised fully-flooded single floe (snow-free sea-ice slab) or a small area of wave slush, both the fraction of ice area affected (f_{w}) and the ice concentration (C) are taken here to be 1.0, and we can compute the melt-rate enhancement by Eq. (6) (Sect. 2.2). In this case, $\mathrm{d}h/\mathrm{d}t \approx 2.9\,\mathrm{cm\,d^{-1}}$.

We next carry out a broader sensitivity analysis of the relative enhancements in daily melt rates ($\mathrm{d}h/\mathrm{d}t$) for the four different classes of wave-modified (-darkened) ice surfaces A-D given in Table 2 (with albedo reductions $\Delta\alpha = 0.38$, 0.48. 0.54, 0.64), and for three wave-flooding and/or wave-slush coverage fractions ($f_{\mathrm{w}} = 0.33$, 0.5, 1.0, based on visual inspection of photographs acquired from icebreakers (Fig. 1a–j)), over November through January and as a function of latitude. Results for 60, 65 and 70° S, i.e., the zone typically covered by sea ice at some time during the annual retreat phase (e.g., Massom et al., 2013), are plotted in Fig. 3. These results and values for the wider latitudinal range of 55–75° S, given in Appendix Tables A1–A3, show that wave-enhanced rates of vertical ice melting steadily build up through November,

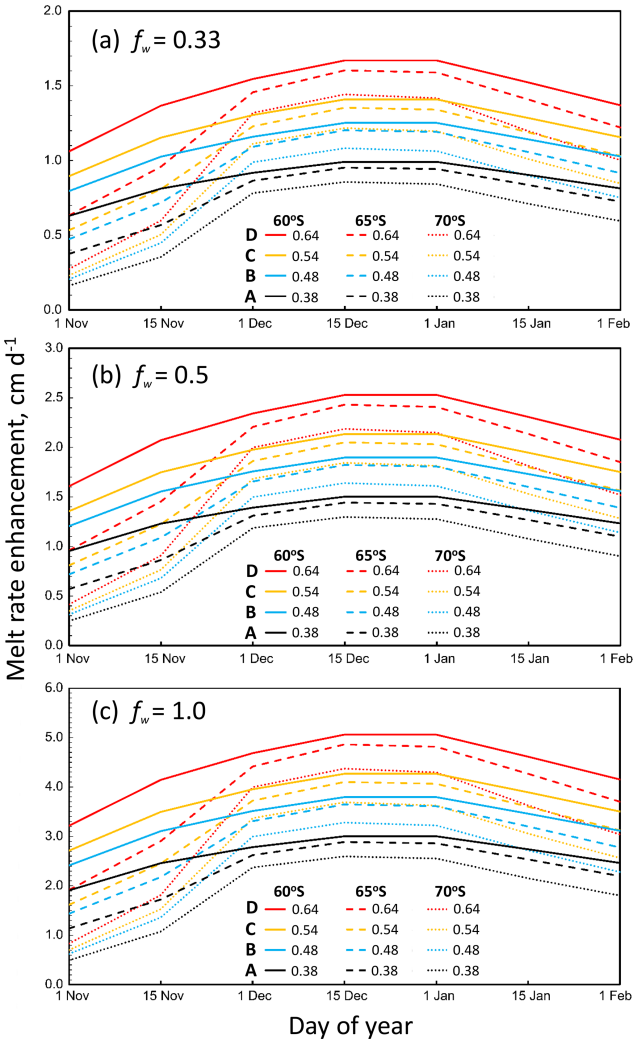

Figure 3. Wave-driven sea-ice melt-rate enhancement ($\mathrm{d}h/\mathrm{d}t$) showing substantial increases in vertical melting (~ 0.2–$5\,\mathrm{cm\,d^{-1}}$ extra) caused by albedo reduction ($\Delta\alpha$) due to wave flooding and/or wave pulverisation. Results are shown for three coverage fractions ($f_\mathrm{w} = 0.33$, 0.5, 1.0) and four surface darkening scenarios (see Table 2) marked A–D in the legend ($\Delta\alpha = 0.38$–0.64) across Antarctic latitudes (60–70° S) during November through January, and for sea ice of density $905\,\mathrm{kg\,m^{-3}}$. Note the different scales on the y axes.

and that they generally increase with decreasing latitude and increasing fraction of coverage. In all cases, values of $\mathrm{d}h/\mathrm{d}t$ converge towards a broad seasonal peak around the December solstice, before slowly decreasing through January.

Estimated values of annual-maximum wave-driven $\mathrm{d}h/\mathrm{d}t$ (in mid-December) for the different wave-darkening and coverage fraction scenarios for three latitudes are shown in Table 3. For ice types A and C which are not greened by algae, vertical melt-rate enhancement ranges from $0.9\,\mathrm{cm\,d^{-1}}$ (for Type A at 70° S where $f_\mathrm{w} = 0.33$) to $4.3\,\mathrm{cm\,d^{-1}}$ (Type C at 60° S where $f_\mathrm{w} = 1.0$), with algal greening increasing these values by 0.2–$0.8\,\mathrm{cm\,d^{-1}}$. There is, in general, a slight decrease in $\mathrm{d}h/\mathrm{d}t$ with increasing latitude south (Tables A1–A3 and Fig. 3), which is steepest in November. Sea-ice coverage south of 70° S is largely confined to the Weddell, Amundsen and Ross seas, whereas sea ice across East Antarctica mainly occurs equatorward of 67° S (Massom et al., 2013). The highest melt-rate enhancements are at 55° S (Tables A1–A3), but sea ice usually attains that latitude only in the eastern limb of the Weddell Gyre at $\sim$5–25° E and parts of East Antarctica around $\sim$80° E, and only in winter through October (cf., Massom et al., 2013; Comiso et al., 2017a).

The values shown in Table 3 are for sea ice with fixed density $905\,\mathrm{kg\,m^{-3}}$ (see Eq. 6), which is taken here to be an approximation for a cold FYI floe. The densities of the four wave-affected ice-surface types are unknown, but they may be lower than $905\,\mathrm{kg\,m^{-3}}$ and are likely to decrease through late-spring and summer as melting progresses and ice permeability and porosity increase. This would be the case if the pore spaces are filled with air, but the density would increase if the pores filled with water. Given these uncertainties, we now investigate the effect of lowering ice density on $\mathrm{d}h/\mathrm{d}t$, using a value of $750\,\mathrm{kg\,m^{-3}}$ measured in Lützow-Holm Bay in East Antarctica by Urabe and Inoue (1988). Results in Table 4 show that decreasing the ice density increases the melt-rate enhancement by an extra 0.1–$1.0\,\mathrm{cm\,d^{-1}}$ compared to ice with density $905\,\mathrm{kg\,m^{-3}}$, pushing $\mathrm{d}h/\mathrm{d}t$ up to 1.0–$6.1\,\mathrm{cm\,d^{-1}}$ (again depending on surface type, latitude, f_w, and greening).

3.4 Potential positive feedback mechanisms that amplify wave melting

We propose that wave-flooding and -pulverisation processes activate a suite of three physical dynamic–thermodynamic positive feedback mechanisms amplified by two physical–biological sub-feedbacks, depicted schematically in Figs. 4 and 5. We argue that these feedbacks should be added to the inventory of feedbacks listed by Goosse et al. (2018). Determining the strengths of the feedbacks is a challenge outside the scope of this paper; our purpose here is to introduce them to stimulate their investigation with targeted observations and modelling, in addition to and in combination with the more-generally-considered ocean–ice albedo feedback.

3.4.1 Wave-driven ice–albedo feedback

Firstly, we hypothesise that wave-driven reductions in albedo will activate a positive sea ice–albedo feedback (Fig. 4) similar to that associated with melt ponds on Arctic sea ice in summer (cf., Curry et al., 1995; Perovich et al., 2009), albeit on different spatial and temporal scales and involving saline wave ponds, wave-washed bare ice and/or wave slush rather than freshwater accumulations formed in floe-surface depressions from melted snow cover. By this "*wave-driven ice–albedo feedback*", the instantaneous decrease in the albedo

Table 3. Estimated annual maximum wave-driven sea-ice vertical melt rate enhancement dh/dt (in cm d^{-1}) on 15 December, for the four wave-affected ice-type classes A–D (see Table 2), three scenarios for the fraction of ice parcel affected ($f_w = 0.33$, 0.5 and 1.0), and three latitudes. Type A is wave-overwashed FYI, wave-compression flooded ice, and/or wave slush; B is green wave slush; C is wave pond; and D is green wave pond and/or green bare ice. Sea-ice density = 905 kg m^{-3}.

Wave-affected surface type	Latitude 60° S			Latitude 65° S			Latitude 70° S		
	$f_w = 0.33$	$f_w = 0.5$	$f_w = 1.0$	$f_w = 0.33$	$f_w = 0.5$	$f_w = 1.0$	$f_w = 0.33$	$f_w = 0.5$	$f_w = 1.0$
A ($\Delta\alpha = 0.38$)	1.0	1.5	3.0	1.0	1.4	2.9	0.9	1.3	2.6
B ($\Delta\alpha = 0.48$)	1.3	1.9	3.8	1.2	1.8	3.6	1.1	1.6	3.3
C ($\Delta\alpha = 0.54$)	1.4	2.1	4.3	1.4	2.1	4.1	1.2	1.8	3.7
D ($\Delta\alpha = 0.64$)	1.7	2.5	5.1	1.6	2.4	4.9	1.4	2.2	4.4

Table 4. Same as Table 3, but for sea-ice density = 750 kg m^{-3}.

Wave-affected surface type	Latitude 60° S			Latitude 65° S			Latitude 70° S		
	$f_w = 0.33$	$f_w = 0.5$	$f_w = 1.0$	$f_w = 0.33$	$f_w = 0.5$	$f_w = 1.0$	$f_w = 0.33$	$f_w = 0.5$	$f_w = 1.0$
A ($\Delta\alpha = 0.38$)	1.2	1.8	3.6	1.1	1.7	3.5	1.0	1.6	3.1
B ($\Delta\alpha = 0.48$)	1.5	2.3	4.6	1.5	2.2	4.4	1.3	2.0	4.0
C ($\Delta\alpha = 0.54$)	1.7	2.6	5.2	1.6	2.5	4.9	1.5	2.2	4.5
D ($\Delta\alpha = 0.64$)	2.0	3.1	6.1	1.9	2.9	5.9	1.7	2.6	5.3

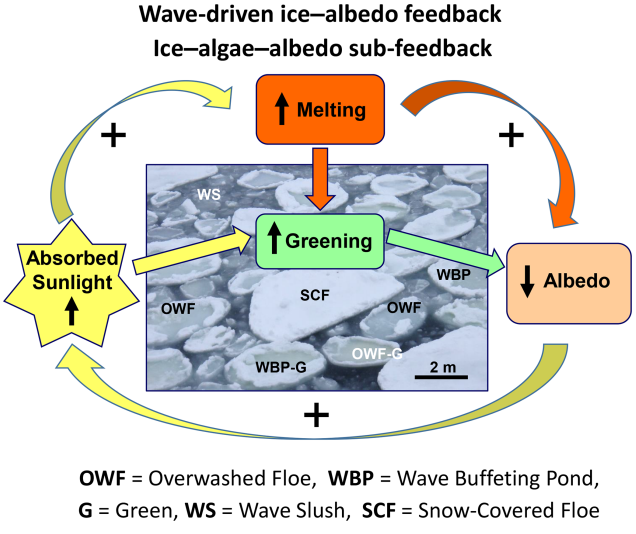

Figure 4. Schematic representation of wave-driven sea ice–albedo feedback, strengthened by wave greening and an embedded ice–algae-albedo sub-feedback. Black up-arrows denote an increase, and black down-arrows a decrease.

of a snow-covered floe caused by the initial wave flooding and/or pulverisation substantially increases the absorption of solar radiation, leading to additional surface and interior melting, which further reduces the ice albedo to then cause additional enhancement of the vertical melt rate, and so on.

3.4.2 Wave greening sub-feedbacks

We further hypothesise that the wave-driven ice–albedo feedback is strengthened in places by two sub-feedbacks associated with wave greening. Firstly, we propose that algal darkening of the ice and/or wave ponds activates what we term an "*ice–algae–albedo sub-feedback*" (Fig. 4), whereby the extra decrease in albedo caused by the onset of wave greening (see Sect. 3.2 and Table 2) further increases the absorption of solar radiation and therefore the vertical melt rate. This melting results in greater light availability for photosynthesis, causing ice algae to proliferate, which further darkens the ice – again an amplifying cycle. We further hypothesise that the two albedo-based feedbacks described above increase the porosity and permeability of affected ice floes as summer progresses, and that this could stimulate additional ice-algal growth and darkening by increasing nutrient replenishment and transport of algae upwards through the more permeable ice column to higher light conditions, to further increase the melt rate and generate additional algal proliferation – and so on. This would entail a positive "*algae–ice permeability sub-feedback*" that further amplifies the ice–algae–albedo sub-feedback. In addition, micro-scale melting around dark algal cells due to their conversion to heat of the enhanced shortwave radiation transmitted (cf., Zeebe et al., 1996) could further increase the ice permeability over time and enhance both the algae–ice permeability sub-feedback and the ice–algae–albedo sub-feedback.

3.4.3 Wave flooding–ice thinning feedback

We further propose that wave-driven thinning lowers the freeboard (surface height above sea level) of small floes,

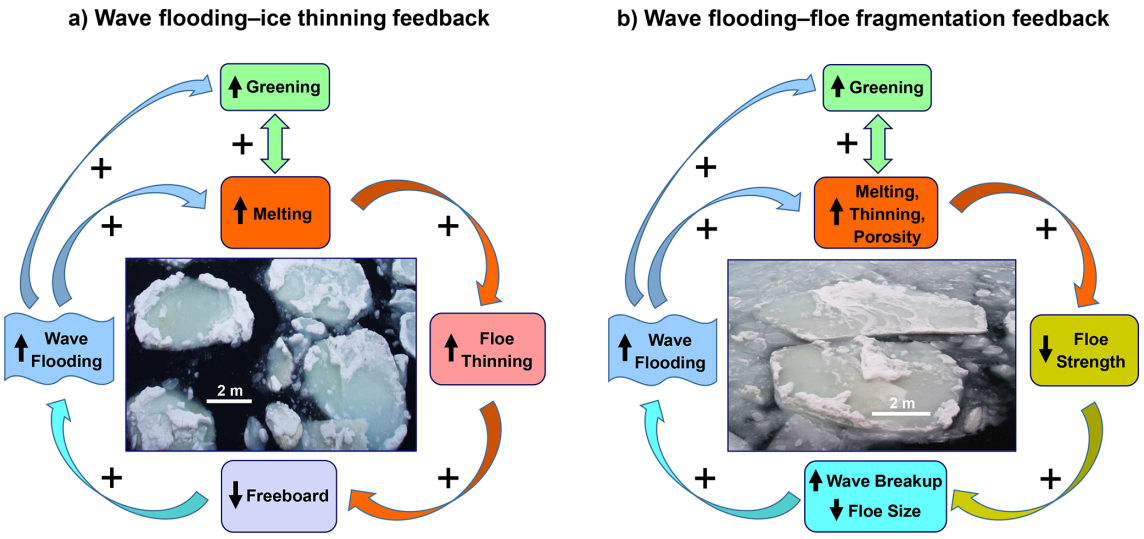

Figure 5. Schematic representations of **(a)** wave flooding–ice thinning feedback, and **(b)** wave flooding–floe fragmentation feedback, both strengthened by positive feedbacks with wave greening as shown. Black up-arrows denote an increase, and black down-arrows a decrease.

which increases their susceptibility to additional wave overwashing and wave ponding. This then increases the wave melting (see Sects. 3.3 and 4.1), leading to further thinning and lowering of the floe freeboard, in an amplifying cycle that we term a "*wave flooding–ice thinning feedback*" (Fig. 5a). The arrow signifying a positive relationship between increased wave flooding and melting shown in Figure 5a includes, and is enhanced by, the wave-driven ice–albedo feedback (Fig. 4) – with the inclusion of the greening box indicating the further enhancement driven in places by the algae-related sub-feedbacks.

3.4.4 Wave flooding–floe fragmentation feedback

We propose that the combined thinning and increase in the porosity of wave-flooded floes would reduce their mechanical strength, i.e., their resistance to compressive and flexural failure (cf., Eicken et al., 1991; Timco and Weeks, 2010), making them more susceptible to further fragmentation by wave flexure into smaller floes which are themselves more susceptible to wave flooding. This results in a "*wave flooding–floe fragmentation feedback*" (Fig. 5b). This feedback is based on the positive relationship between the strength of a sea-ice "slab" and its thickness (Chai et al., 2020), and the negative relationship between sea-ice strength and porosity (Timco and Weeks, 2010; Wang et al., 2022; Mellor, 1986; Eicken et al., 1991). At the same time, it is influenced by, and contributes to, the wave flooding–ice thinning feedback, and is coupled to the other feedbacks described above.

The wave flooding–floe fragmentation feedback would also enhance the ocean–ice albedo feedback (cf., Nihashi and Cavalieri, 2006), by helping to create smaller floes that are more mobile than large floes and have a larger perimeter per unit area, thereby promoting lateral and basal melting in summer. The increased mobility of these smaller floes may also increase their likelihood of drifting northwards under Ekman divergence driven by winds and/or ocean eddies (cf., Auger et al., 2023), i.e., into warmer and wavier waters.

4 Discussion

4.1 Wave-driven enhancement of sea-ice melting

Our initial results – based on limited point observations and simple one-dimensional modelling of a single floe or parcel of wave slush – indicate that the flooding and pulverisation of sea-ice floes by waves can substantially influence the solar energy budget of parts of the SIZ. Removal or wetting of snow, seawater ponding and creation of wave slush are estimated to reduce the albedo of an original floe of snow-covered FYI by as much as 0.54. This causes a large increase in the absorption of solar radiation by the ice in spring through summer, enhancing the vertical melt-rate by an extra 0.9–4.3 $\mathrm{cm\,d^{-1}}$ compared to a snow-covered first-year floe and depending on the fraction of ice area flooded/pulverised, latitude and time of year. We hypothesise that this wave-driven surface and interior melting supplements the conventionally-considered lateral and basal melting.

Concurrently, we propose that wave flooding and wave-pulverisation processes, and resultant snow removal, produce suitable high-light and high-nutrient habitats for low-light-adapted ice algae within the ice column, wave ponds and wave slush. We speculate that the enhanced primary production would further decrease the albedo by 0.1, to push $\Delta\alpha$ to 0.64. This would increase the vertical melt-rate enhancement to 1.1–5.1 $\mathrm{cm\,d^{-1}}$, meaning that wave melting ampli-

fied by wave greening could completely melt a 1 m-thick slab of wave-flooded ice in just 20 d (assuming no other contributing factors). The melt-rate enhancement increases to up to 6.1 cm d^{-1} if the floe density is assumed to be lower at 750 kg m^{-3}, as found in some measurements. In addition, the melt-rate enhancement of unconsolidated wave slush could be even greater, given the much smaller particles of ice involved, and their continual churning by passing waves and contact with warming seawater.

While this preliminary study is limited to instantaneous modelling of daily wave-melting only, we propose that our initial estimates of the melt-rate enhancements are probably underestimates, because of five previously-unconsidered coupled positive feedbacks and sub-feedbacks that link physical and biological processes. In addition, the intensified transmittance of solar radiation through wave-flooded and wave-ponded ice "skylights" could heat the ocean mixed layer (cf., Nicolaus et al., 2010), to enhance the basal and lateral melting of floes – as is the case for melt ponds in the Arctic (Inoue et al., 2008). Although no Antarctic measurements are available, Arctic observations show that freshwater melt ponds there increase the amount of shortwave radiation transmitted through the ice in summer by up to about a factor of four (Nicolaus et al., 2012; Light et al., 2015). Arctic melt-pond transmittance attains values of 0.5 compared to ~ 0.2 for bare ice and ~ 0.0–0.1 for snow-covered ice (Perovich, 2005), leading to melt rates under ponds that are 2–3 times higher than they are for bare ice (Fetterer and Untersteiner, 1998; Perovich et al., 2003).

There are two other ways in which wave-flooding and wave-pulverisation processes may contribute to surface melting in summer. First, wave overwashing would directly cause surface melting of small floes swept northwards from the pack-ice zone into warmer waters. Second, removal of the insulating snow buffer by waves directly exposes bare floe surfaces and/or wave slush to direct melting by air temperatures above 0 °C as summer progresses.

4.2 Large-scale spatio-temporal influence of wave melting

A number of factors point to wave melting likely making a significant contribution to driving the melt phase of Antarctica's climatological annual sea-ice cycle when combined and integrated over the entire SIZ. Not least is the vast circumpolar extent of the MIZ (Brouwer et al., 2022; Day et al., 2024) and its constant interaction with both large ocean swells (cf., Young et al., 2020) and wind waves locally generated by intense cyclones (Vichi et al., 2019; Alberello et al., 2022).

For ice-edge zones compacted by on-ice winds (e.g., Massom et al., 2008), attenuation of wave energy by the high-concentration ice cover (e.g., Squire, 2020) is likely to limit wave overwashing and wave pulverisation to a relatively short distance in from the ice edge (Pitt et al., 2022). However, the Antarctic ice-edge zone is typically more diffuse (e.g., see Fig. 1 of Massom and Stammerjohn, 2010) due to the frequent passage of storms (cf., Simmonds et al., 2003) and the occurrence of ocean eddies (cf., Auger et al., 2023; see also Fig. 9 of Massom et al., 1999). In particular, the areal influence of wave melting – and the feedbacks and sub-feedbacks proposed in Sect. 3.4 – is likely to be substantially extended in late-spring through summer by the widespread occurrence of fields of elongated bands of floes driven by off-ice winds away from the main SIZ and into more open-ocean conditions, where they wave-fracture into smaller floes (Comiso et al., 1992; Wadhams, 2000; Ishida and Ohshima, 2009) that are more susceptible to wave overwashing (snow removal) and wave ponding. Such bands, which are separated by open water, can be a few tens of metres to kilometres wide and can extend over zones ranging from about 100 km (Saiki and Mitsudera, 2016) to >300 km wide (Massom and Stammerjohn, 2010). The fraction of ice surface covered by wave overwashing and ponding (i.e., f_w) can be particularly high in ice-edge bands, e.g., $\sim 50\,\%$–$60\,\%$ in the narrow band in Fig. 1d.

In addition, we hypothesise that seasonal wave-melting is not confined to the MIZ, but that it also occurs within the interior Antarctic SIZ due to (1) the presence there of extensive open-water areas in the form of large leads (cf., Dubey et al., 2025) and both coastal and offshore polynyas (cf., Barber and Massom, 2007) and (2) the occurrence of deep swell-penetration events. Under the first scenario proposed, locally-generated wind waves drive localised ice flooding, pulverisation and greening around the lead and polynya margins (see Sect. 3.1.1), with the resultant wave melting increasing as the melt season progresses and the open-water areas expand rather than freeze over, to potentially contribute to the seasonal meltback of the SIZ from within (cf., Massom et al., 2003). Secondly and under certain circumstances, it is possible that the propagation of swells deep into the pack drives wave flooding there. Wave-compression flooding (Sect. 3.1.3) has been observed in the compact inner East Antarctic SIZ up to 360 km south of the sea-ice edge, e.g., Fig. 1g, h (also Massom et al., 1999). In the Weddell Sea in winter 1986, a series of waves of 18 s period and 1 m amplitude caused active ridging and rafting of the ice cover (concentration 90 % and average thickness 0.8 m) at 560 km in from the ice edge (Liu and Mollo-Christensen, 1988), to potentially cause deformation ponding. More observations are required to validate the occurrence of wave melting within the interior SIZ (i.e., during deep wave penetration events and adjacent to leads and polynyas), and to determine their overall contribution to the observed seasonal meltback of the Antarctic SIZ.

Another factor that likely enhances the occurrence and influence of wave melting is the nature of the sea-ice cover itself. Antarctic first-year and younger floes are relatively thin and typically have a near-zero or negative freeboard (Worby et al., 1998) due in large part to the weight of the overly-

ing snow cover (Massom et al., 2001). As such, they are naturally vulnerable to wave overwashing and wave ponding (see Fig. 1a–f), although large waves will also overwash floes with higher freeboard.

5 Conclusions and outlook

In this preliminary study, we have expanded upon the classical picture that late spring–summer melting of Antarctic sea ice occurs by lateral and basal melting accelerated by a positive ocean–ice albedo feedback (e.g., Horvat, 2022) accentuated by the wave-driven breakup of floes in the MIZ – by providing evidence that waves also drive rapid ice surface (and interior) melting that has been neglected to date. We propose that wave flooding and wave pulverisation remove the thermal and optical buffer provided by snow cover and/or mechanically grind down floes into wave slush and also create optimal habitat for proliferation of ice algae (wave greening) – not only in the MIZ but also in the interior SIZ.

5.1 Albedo reduction

With simple one-dimensional modelling based on proxy estimates of wave-modified ice albedo, we show that the wave-driven reduction in sea-ice albedo is as much as 0.54, and that this enhances the vertical melt-rate by up to an extra $4.3\,\mathrm{cm\,d^{-1}}$ (compared to a snow-covered first-year floe). We also propose that wave greening decreases the albedo by an additional 0.1 to a combined reduction of 0.64, to amplify the wave-driven melt enhancement to as much as $5.1\,\mathrm{cm\,d^{-1}}$, and as much as $6.1\,\mathrm{cm\,d^{-1}}$ if the floe density is taken to be $750\,\mathrm{kg\,m^{-3}}$ (rather than $905\,\mathrm{kg\,m^{-3}}$). Not only this, but we also propose that wave flooding, pulverisation and greening activate five coupled positive feedbacks and sub-feedbacks that potentially further accelerate the melt-rate enhancement as summer progresses.

5.2 Wave ponding

In the Arctic, there has been strong recognition of the need for explicit or implicit treatment of melt ponds in climate and Earth system models (e.g., Taylor and Feltham, 2004; Flocco et al., 2010; Tsamados et al., 2015; Webster et al., 2022; Diamond et al., 2023), in order to simulate Earth's radiation balance (Maslanik et al., 2007; Perovich et al., 2008; Nicolaus et al., 2010) and the strength of the ice–albedo feedback (Curry et al., 1995, 2001; Tschudi et al., 2008). Results presented here suggest that the same recognition and parameterisation in models is required for wave-overwashed floes, saline wave ponds, wave slush and wave greening and associated feedbacks in the Antarctic (and the Arctic). However, there are fundamental differences. Unlike Arctic melt ponding, wave flooding and wave pulverisation (in the Antarctic and the Arctic) are not limited to the warm season but rather occur year-round. Although wave-melting processes may influence a small proportion of the overall SIZ at the start of the melt season, the proportion affected is likely to increase as the SIZ recedes through summer. Wave melting also has implications for the ocean freshwater budget and upper-ocean buoyancy and stratification, which would feed back to influence sea-ice formation and melt.

5.3 The marginal ice zone

Given the factors highlighted in this paper, it is likely that wave-melting processes contribute to: (1) the observed predominant role of the MIZ in driving overall mean annual sea-ice retreat around Antarctica (cf., Kimura et al., 2022); and (2) the observed close spatio-temporal correspondence between (trends in) significant wave height and circum-Antarctic sea-ice extent and annual retreat identified by Kohout et al. (2014). Our initial findings further support the assertion that the Antarctic SIZ is vulnerable to increased storminess (Kohout et al., 2014), but add wave flooding and greening and associated feedbacks as processes that need to be considered in addition to the generally-considered wave fragmentation of floes. Moreover, we highlight that the mechanical breakdown of floes in the MIZ occurs not only by wave-driven flexural fracture (Williams et al., 2013) but also by the wave-driven pulverisation of floes and their snow cover into wave slush (see Sect. 3.1.4). As a result, low-albedo wave slush between small floes and brash ice may form a significant portion of the sea-ice cover in the outer MIZ, as shown locally in Fig. 1i, j, although this is again yet to be established and quantified on the large-scale. Notwithstanding this caveat, the new paradigm challenges the commonly-held view that the MIZ in late spring–summer is simply a collection of wave-fractured small (snow-covered) floes that decrease in size with increasing proximity to the ice edge (open ocean) and are either closely packed or separated by open water (depending on wind direction). Another unknown factor worthy of investigation is that unconsolidated fields of wave-slush particles (and small brash-ice fragments) are susceptible to particularly rapid seasonal melting (compared to floes) due to their small size and their direct contact with wave-driven pulsations of warm seawater (driven by wave churning) in summer – with this melt enhancement of wave slush again being increased by wave greening (cf., Massom et al., 2006).

Ice-edge bands have been considered to influence the seasonal ablation of the MIZ, e.g., in the Arctic (Martin et al., 1983), by increasing the open-water area within the pack and by enhancing wave-driven flexural breakup of the ice into smaller floes, which promotes rapid lateral and basal melting of floes within the outer MIZ (Saiki and Mitsudera, 2016). To this, we add the influence of wave melting processes on floes within the bands themselves, and hypothesise that bands (and ice-edge ocean eddies) extend the spatial domain of wave-melting influence – including smaller bands such as that in Fig. 1d.

5.4 Biology

Another factor highlighted here is that wave greening contributes to: (1) overall primary production within the Antarctic SIZ (cf., Saenz and Arrigo, 2014; Dalman et al., 2025) including the MIZ (cf., Taylor et al., 2013); and (2) phytoplankton blooms seaward of the ice edge as it retreats (Massom et al., 2006; cf., Arrigo et al., 2014) and within polynyas (cf., Arrigo and van Dijken, 2003) in late-spring through summer. While we have proposed that snow-free wave-flooded floes and wave-pulverised slush fields form hotspot habitats for intra-ice algal proliferation and blooms in spring–summer, they also potentially support active communities of low-light-adapted algae and elevated chlorophyll concentrations before the September equinox, and even in winter in the Antarctic MIZ (cf., Louw et al., 2022) when the ice reaches relatively-low latitudes of $\sim$ 57–60° S in places. Neither are detectable in satellite ocean-colour imagery and therefore remain neglected and unquantified in estimates of Southern Ocean primary production within the SIZ (cf., Massom et al., 2006). Moreover, transmittance of shortwave radiation through skylights in wave-flooded floes and wave-slush likely facilitates and contributes to the formation of under-ice blooms (cf., Arrigo et al., 2012; Hague and Vichi, 2021; Horvat et al., 2022), i.e., indirect wave greening. At the same time, wave melting and wave pulverisation likely increase the release of algae and other biogenic material into the upper ocean and its availability for under-ice pelagic grazers in the MIZ year round and at the receding ice edge in late spring–summer, to support high concentrations of higher trophic levels there (Massom et al., 2006).

5.5 Carbon and clouds

Wave greening would additionally contribute to key biogeochemical processes – with implications for marine ecosystems, properties of the Southern Ocean, and weather and climate – including (1) the uptake by the Southern Ocean of anthropogenic carbon from the atmosphere to help moderate climate warming (cf., Frölicher et al., 2015); (2) the marine biological carbon pump (cf., Henley et al., 2020); and (3) ice-algal production of cloud-condensation nuclei (cf., Mallet et al., 2025). Clouds formed in this way then influence the surface radiation and energy balances (Tison et al., 2017) and precipitation – to affect sea-ice conditions and algal production, and so on in a possible feedback (cf., Charlson et al., 1987; Wang et al., 2018).

5.6 Remote sensing

Another influence of wave flooding and wave pulverisation requiring investigation and quantification is on the accuracy of sea-ice concentration (and extent) retrievals from satellite passive-microwave brightness temperature data in wave-flooded and -pulverised areas (Massom et al., 1999; and cf., Comiso et al., 1992 and Ivanova et al., 2015). For example, the scenes shown in Fig. 1a, g and i–j have ice covers with 100 % concentration, but this value is likely to be substantially underestimated in standard satellite passive-microwave sea-ice concentration products from the MIZ (and year-round) as the microwave emissivity of flooded ice and/or wave slush is intermediate between that of cold FYI with a dry snow cover and open water (cf., Comiso and Steffen, 2001). Any such underestimate of ice-concentration has implications for the monitoring of sea-ice extent and area and analysis of their trends in the long-term satellite dataset dating back to 1979 (cf., Lubin and Massom, 2006). In addition, wave flooding and wave pulverisation, and their likely effects on ice density and snow-cover properties, need accounting for in the estimation of both sea-ice and snow-cover thickness from satellite radar and laser altimeter measurements in the MIZ and adjacent to large leads and polynyas (cf., Kacimi and Kwok, 2020).

5.7 The Arctic

While our focus has been on Antarctic sea ice, the same wave processes and feedbacks also apply to the Arctic (e.g., Massom, 1991) – and not only in marginal seas but also in the central Arctic Ocean where wave-ice interaction processes occur (cf., Squire et al., 2009). In the Northern Hemisphere, loss of sea-ice coverage (particularly in summer, e.g., Comiso et al., 2017b) has exposed the Arctic Ocean to more swells (Thomson and Rogers, 2014), to increase the likelihood of more extensive wave flooding and pulverisation there and resultant wave melting. This could in turn lead to wave greening, which is likely to be less intense in conventional freshwater melt ponds due to relative lack of nutrients limiting primary production therein (cf., Sørensen et al., 2017).

5.8 The future

Around Antarctica, wave flooding, pulverisation, greening and melting may already be intensifying, given observed increases in recent decades in: (i) cyclones at high southern latitudes related to a poleward shift in storm tracks (IPCC, 2014), and (ii) both wave height and near-surface wind speed over the Southern Ocean adjacent to the SIZ (Young and Ribal, 2019; Morim et al., 2019). Looking to the future, wave greening and melting of the Antarctic SIZ will likely increase in coming decades, given predicted further increases in wind speed and wave height across the high-latitude Southern Ocean (Casas-Prat et al., 2024; Liu et al., 2024). This intensification would contribute to changing the thickness and properties of the ice and its snow cover (cf., Webster et al., 2018) and melt rates but potentially also ice formation rates – to impact the seasonality and extent of both the seasonal pack-ice zone (cf., Stammerjohn et al., 2012) and the coastal fast-ice zone (cf., Fraser et al., 2023). This would in turn affect: planetary albedo and polar amplification (cf., Riihelä et al.,

2021; Goosse et al., 2023); oceanic and atmospheric interactions, properties and circulation, and the ocean and global freshwater budget (cf., Haumann et al., 2016; Meredith and Brandon, 2017; Smith et al., 2017; England et al., 2018); low-latitude and global weather and climate (cf., England et al., 2020; Ayres et al., 2022); the stability of the Antarctic ice shelves, ice-sheet mass loss and sea-level rise (cf., Massom et al., 2018; Teder et al., 2025); marine ecosystem structure and function, health and biodiversity (cf., Massom and Stammerjohn, 2010; Ducklow et al., 2013; Meredith et al., 2022); the capacity of the Southern Ocean to take up atmospheric carbon and to moderate anthropogenic climate change (cf., Williams et al., 2023), while also influencing ocean acidification (cf., Nissen et al., 2024); and other biogeochemical processes that feed back into the climate system (cf., Vancoppenolle et al., 2013). These potential scenarios underline the need to better understand and quantify wave melting and greening processes and feedbacks and their overall pan-Antarctic influence, towards their inclusion in Earth system models.

6 Recommendations for measurements and follow-on work

The new paradigm presented here is based on limited observations and simple modelling only, with sensitivity analysis of daily wave-driven vertical melt-rate enhancement ($\mathrm{d}h/\mathrm{d}t$) of a single floe and/or parcel of wave slush as a function of latitude, time in summer and proportion of the ice surface affected. An important next step is to carry out targeted observations in order to quantify the larger-scale coverage and influence of wave flooding, wave pulverisation, wave greening and wave melting, and their spatio-temporal distribution and variability as a function of swell and wind-wave conditions, ice conditions (floe size and ice type, thickness and concentration), and distance from the ice edge. Obtaining estimates of these quantities across the MIZ and the wider SIZ (including within leads and polynyas) is challenging, given the scale and dynamism of the environment involved. It will require coordinated use of autonomous technologies such as ship-borne stereo camera systems (e.g., Alberello et al., 2022) and arrays of wave and ice mass-balance buoys, and remotely-piloted vehicle remote sensing (including hyperspectral sensors to detect and quantify wave greening) – extended in space and time using satellite high-resolution remote sensing (including synthetic aperture radar e.g., Gebhardt et al., 2016; Stopa et al., 2018) combined with novel altimetric measurement of wave penetration distances into the SIZ that may be able to detect deep swell-penetration (e.g., Brouwer et al., 2022; Fraser et al., 2026) and wave reanalysis information.

Additional unknowns in need of measurement and modelling include: (1) the properties and wave-melting behaviour of wave slush; and (2) the extra contribution of wave flooding to enhancing ice-floe lateral and basal melting and its associated ocean–ice albedo feedback (cf., Nihashi and Cavalieri, 2006) via increasing the transmittance of shortwave radiation through the ice (cf., Nicolaus et al., 2012). More work is also required to investigate, model and quantify the role of ice-edge banding (and eddies) in extending wave flooding, pulverisation, greening and melting, and to determine how banding distribution, composition (floe size and wave slush proportion) and processes respond to changing wind and wave conditions. Also in need of investigation and quantification is the direct influence of wave overwashing on surface melting where bands (and ocean eddies) isolate floes from the main pack and transport them equatorward into warmer waters.

Targeted ship-based and in situ spectral radiation measurements are needed to quantify the albedo and transmittance of the different wave-affected surfaces, including the effects of algal greening. Also needed are coincident detailed in situ observations and sampling of the following and their evolution in space and time:

- the thickness, morphology, density, salinity and brine volume, temperature and micro-structural properties (e.g., porosity and permeability) of wave-flooded floes and wave slush, and the depth and characteristics of wave ponds;
- their algal pigment content and community composition, primary production and nutrients; and
- their role in key biogeochemical processes within and under the SIZ (cf., Henley et al., 2020), and notably the ocean biological carbon pump and the uptake of atmospheric CO_2 by the ocean (cf., Hauck et al., 2015) and the production by ice algae of climate-active sulphur-compound gases (cf., Trevena and Jones, 2006).

In parallel, targeted modelling efforts are required to both synthesise the observations and carry out sensitivity analyses, to determine (1) the extra contribution of wave flooding and pulverisation to enhancing ice-floe lateral and basal melting via increasing the transmittance of shortwave radiation through the ice (cf., Nicolaus et al., 2012), and (2) the pan-Antarctic contribution of wave melting to the rapid melt phase of the annual sea-ice cycle. For the modelling, a particular challenge will be to parameterise the coupled feedbacks described here, and to quantify their role in accelerating wave melting under a range of sea-ice and wave conditions. The ultimate aim is to encourage inclusion of wave-melting processes, associated albedo modification (change) and feedbacks in coupled climate and Earth system models, as a crucial step towards (1) the more accurate simulation of the climatological annual cycle of Antarctic sea ice and its current state; (2) attributing observed recent high variability in the Southern Ocean sea-ice system; and (3) more robust prediction of the future fate of both polar sea-ice systems and the wider Earth system.

Appendix A

Table A1. Estimated values of wave-driven sea-ice vertical melt-rate enhancement dh/dt (in cm d^{-1}) for the four wave-affected classes A–D (see Table 2) where $f_w = 0.33$, as a function of change in albedo ($\Delta\alpha = 0.64$, 0.54, 0.48 and 0.38), latitude (55–75° S) and day of year (1 November–1 February). Sea-ice density = 905 kg m^{-3}. Values for 60, 65 and 70° S are plotted in Fig. 3a.

D ($\Delta\alpha = 0.64$)	1 Nov	15 Nov	1 Dec	15 Dec	1 Jan	15 Jan	1 Feb
55° S	1.2	1.5	1.6	1.7	1.7	1.5	1.5
60° S	1.1	1.4	1.5	1.7	1.7	1.5	1.4
65° S	0.6	1.0	1.5	1.6	1.6	1.4	1.2
70° S	0.3	0.6	1.3	1.4	1.4	1.2	1.0
75° S	0.2	0.6	1.3	1.5	1.5	1.3	1.0
C ($\Delta\alpha = 0.54$)	1 Nov	15 Nov	1 Dec	15 Dec	1 Jan	15 Jan	1 Feb
55° S	1.1	1.3	1.3	1.5	1.5	1.3	1.2
60° S	0.9	1.2	1.3	1.4	1.4	1.3	1.2
65° S	0.5	0.8	1.2	1.4	1.3	1.2	1.0
70° S	0.2	0.5	1.1	1.2	1.2	1.0	0.8
75° S	0.1	0.5	1.1	1.2	1.3	1.1	0.8
B ($\Delta\alpha = 0.48$)	1 Nov	15 Nov	1 Dec	15 Dec	1 Jan	15 Jan	1 Feb
55° S	0.9	1.1	1.2	1.3	1.3	1.2	1.1
60° S	0.8	1.0	1.2	1.3	1.3	1.1	1.0
65° S	0.5	0.7	1.1	1.2	1.2	1.1	0.9
70° S	0.2	0.4	1.0	1.1	1.1	0.9	0.8
75° S	0.1	0.5	1.0	1.1	1.1	1.0	0.7
A ($\Delta\alpha = 0.38$)	1 Nov	15 Nov	1 Dec	15 Dec	1 Jan	15 Jan	1 Feb
55° S	0.7	0.9	0.9	1.0	1.0	0.9	0.9
60° S	0.6	0.8	0.9	1.0	1.0	0.9	0.8
65° S	0.4	0.6	0.9	1.0	0.9	0.8	0.7
70° S	0.2	0.4	0.8	0.9	0.8	0.7	0.6
75° S	0.1	0.4	0.8	0.9	0.9	0.8	0.6

Table A2. Estimated values of wave-driven sea-ice vertical melt-rate enhancement dh/dt (in cm d^{-1}) for the four wave-affected classes A–D (see Table 2) where $f_w = 0.5$, as a function of change in albedo ($\Delta\alpha = 0.64$, 0.54, 0.48 and 0.38), latitude (55–75° S) and day of year (1 November–1 February). Sea-ice density = 905 kg m^{-3}. Values for 60, 65 and 70° S are plotted in Fig. 3b.

D ($\Delta\alpha = 0.64$)	1 Nov	15 Nov	1 Dec	15 Dec	1 Jan	15 Jan	1 Feb
55° S	1.9	2.3	2.4	2.6	2.6	2.3	2.2
60° S	1.6	2.1	2.3	2.5	2.5	2.3	2.1
65° S	1.0	1.5	2.2	2.4	2.4	2.1	1.8
70° S	0.4	0.9	2.0	2.2	2.1	1.8	1.5
75° S	0.3	1.0	2.0	2.2	2.3	2.0	1.5
C ($\Delta\alpha = 0.54$)	1 Nov	15 Nov	1 Dec	15 Dec	1 Jan	15 Jan	1 Feb
55° S	1.6	1.9	2.0	2.2	2.2	2.0	1.9
60° S	1.4	1.7	2.0	2.1	2.1	1.9	1.8
65° S	0.8	1.2	1.9	2.1	2.0	1.8	1.6
70° S	0.4	0.8	1.7	1.8	1.8	1.5	1.3
75° S	0.2	0.8	1.7	1.9	1.9	1.7	1.3
B ($\Delta\alpha = 0.48$)	1 Nov	15 Nov	1 Dec	15 Dec	1 Jan	15 Jan	1 Feb
55° S	1.4	1.7	1.8	2.0	2.0	1.8	1.7
60° S	1.2	1.6	1.8	1.9	1.9	1.7	1.6
65° S	0.7	1.1	1.7	1.8	1.8	1.6	1.4
70° S	0.3	0.7	1.5	1.6	1.6	1.4	1.1
75° S	0.2	0.7	1.5	1.7	1.7	1.5	1.1
A ($\Delta\alpha = 0.38$)	1 Nov	15 Nov	1 Dec	15 Dec	1 Jan	15 Jan	1 Feb
55° S	1.1	1.3	1.4	1.5	1.5	1.4	1.3
60° S	1.0	1.2	1.4	1.5	1.5	1.4	1.2
65° S	0.6	0.9	1.3	1.4	1.4	1.3	1.1
70° S	0.2	0.5	1.2	1.3	1.3	1.1	0.9
75° S	0.2	0.6	1.2	1.3	1.3	1.2	0.9

Table A3. Estimated values of wave-driven sea-ice vertical melt-rate enhancement dh/dt (in cm d^{-1}) for the four wave-affected classes A–D (see Table 2) where $f_w = 1.0$, as a function of change in albedo ($\Delta\alpha = 0.64$, 0.54, 0.48 and 0.38), latitude (55–75° S) and day of year (1 November–1 February). Sea-ice density = 905 kg m^{-3}. Values for 60, 65 and 70° S are plotted in Fig. 3c.

D ($\Delta\alpha = 0.64$)	1 Nov	15 Nov	1 Dec	15 Dec	1 Jan	15 Jan	1 Feb
55° S	3.8	4.5	4.8	5.2	5.2	4.7	4.4
60° S	3.2	4.1	4.7	5.1	5.1	4.6	4.1
65° S	1.9	2.9	4.4	4.9	4.8	4.3	3.7
70° S	0.8	1.8	4.0	4.4	4.3	3.6	3.0
75° S	0.5	1.9	4.1	4.4	4.5	4.0	3.0
C ($\Delta\alpha = 0.54$)	1 Nov	15 Nov	1 Dec	15 Dec	1 Jan	15 Jan	1 Feb
55° S	3.2	3.8	4.1	4.4	4.4	4.0	3.8
60° S	2.7	3.5	4.0	4.3	4.3	3.9	3.5
65° S	1.6	2.5	3.7	4.1	4.1	3.6	3.1
70° S	0.7	1.5	3.4	3.7	3.6	3.1	2.6
75° S	0.4	1.6	3.4	3.7	3.8	3.4	2.6
B ($\Delta\alpha = 0.48$)	1 Nov	15 Nov	1 Dec	15 Dec	1 Jan	15 Jan	1 Feb
55° S	2.8	3.4	3.6	3.9	3.9	3.5	3.3
60° S	2.4	3.1	3.5	3.8	3.8	3.5	3.1
65° S	1.4	2.2	3.3	3.6	3.6	3.2	2.8
70° S	0.6	1.4	3.0	3.3	3.2	2.7	2.3
75° S	0.4	1.4	3.0	3.3	3.4	3.0	2.3
A ($\Delta\alpha = 0.38$)	1 Nov	15 Nov	1 Dec	15 Dec	1 Jan	15 Jan	1 Feb
55° S	2.2	2.7	2.9	3.1	3.1	2.8	2.6
60° S	1.9	2.5	2.8	3.0	3.0	2.7	2.5
65° S	1.1	1.7	2.6	2.9	2.9	2.5	2.2
70° S	0.5	1.1	2.4	2.6	2.6	2.2	1.8
75° S	0.3	1.1	2.4	2.6	2.7	2.4	1.8

Code availability. The repository (https://doi.org/10.5281/zenodo.18995070, Reid, 2026) contains all scripts necessary to reproduce final Fig. 3 and the estimates of wave-driven melt-rate enhancements given in the tables.

Data availability. The data used to generate final Fig. 3 in this study are available at: https://doi.org/10.5281/zenodo.18995070 (Reid, 2026). The record and files are publicly accessible. Output data are given in Tables A1–A3.

Author contributions. RAM conceptualised the study and carried out the visual observations of the wave processes and phenomena. SGW, BL and DKP provided albedo data and surrogate albedo values; SGW designed the surface radiation energy budget calculation; PAR developed the model code, ran the model and provided the model output and Fig. 3; RAM, PAR and SGW analysed the output; and RAM conceptualised the feedbacks. LGB, MHM, AT and GP provided expert input on wave-ice interaction; PU, SPO, PAR and PGS on sea-ice modelling; KMM, PGS and PW on sea-ice algae; and ADF, PW, SMTC and MF on remote sensing. RAM prepared the manuscript with contributions from all co-authors.

Competing interests. At least one of the (co-)authors is a member of the editorial board of *The Cryosphere*. The peer-review process was guided by an independent editor, and the authors also have no other competing interests to declare.

Disclaimer. Publisher's note: Copernicus Publications remains neutral with regard to jurisdictional claims made in the text, published maps, institutional affiliations, or any other geographical representation in this paper. The authors bear the ultimate responsibility for providing appropriate place names. Views expressed in the text are those of the authors and do not necessarily reflect the views of the publisher.

Acknowledgements. RAM is very grateful to the Australian, US and German Antarctic programs and the masters and crews of the icebreakers RVs *Aurora Australis*, *Nathaniel B Palmer* and *Polarstern*, and to Drs Ray Smith and Sharon Stammerjohn for enabling his participation in the US National Science Foundation Palmer LTER program. SGW thanks the Institute for Marine and Antarctic Studies (IMAS) for their hospitality during visits to Hobart to work on this paper. We gratefully acknowledge the US National Snow and Ice Data Center for the satellite sea-ice concentration data used in this study. We sincerely thank Dr. Clare Eayrs and two anonymous reviewers for their detailed, insightful and highly-constructive reviews which have substantially strengthened the paper, and also thank the editor Dr. Stephen Howell.

Financial support. This work was funded by, and contributes to, Australian Antarctic Science project nos. 4073, 4116, 4123, 4298, 4506, 4625 and 4635. RAM and KMM are supported by the Australian Antarctic Division (AAD), and received grant funding from the Australian Government as part of the Antarctic Science Collaboration Initiative program (grant no. ASCI000002), the Australian Research Council Special Research Initiative the Australian Centre for Excellence in Antarctic Science (ACEAS, project no SR200100008), and the Australian Research Council's Special Research Initiative for Antarctic Gateway Partnership (project no. SR140300001). PAR is supported by the Australian Bureau of Meteorology and received grant funding from the Australian Government as part of the Antarctic Science Collaboration Initiative program (grant no. ASCI000002). LGB is funded by the Australian Research Council (grant nos. FT190100404, DP240100325), and ACEAS (project no. SR200100008). PU is funded by the European Union Horizon 2020 PolarRES project (grant no. 101003590) and by the Research Council of Finland (grant no. 364876). For DKP, this work was supported by US National Oceanic and Atmospheric Administration project NA24OARX431G0018 and US National Science Foundation (NSF) project NSF-OPP-2138785. BL gratefully acknowledges financial support from the US Office of Naval Research (grant no. N00014-23-1-2484) and NSF (ARCSS 2138787 and Arctic Natural Sciences 2143547). AT acknowledges support from the Australian Research Council (grant nos. LE220100103, DP240100325). ADF is supported by the Australian Research Council (grant nos. FT230100234, LP170101090, LE220100103 and DP240100325) and, with PW, received grant funding from the Australian Government as part of the Antarctic Science Collaboration Initiative program (grant no. ASCI000002) and from the Harris Charitable Trust through the Antarctic Science .Foundation. PW is also supported by the AAD and received grant funding from the Australian Government as part of the Antarctic Science Collaboration Initiative program (grant no. ASCI000002). SMTC is supported by the AAD and received grant funding from the Australian Government as part of the Antarctic Science Collaboration Initiative program (grant no. ASCI000002) and from the International Space Science Institute team grant no. 501. MF is supported by AAD. PGS is supported by the Australian Research Council Special Research Initiative the Australian Centre for Excellence in Antarctic Science (ACEAS, project no SR200100008) and the Centre for Excellence for 21st Century Weather (grant no. CE230100012).

Review statement. This paper was edited by Stephen Howell and reviewed by Clare Eayrs and two anonymous referees.

References

Abram, N. J., Purich, A., England, M. H., McCormack, F. S., Strugnell, J. M., Bergstrom, D. M., Vance, T. R., Stål, T., Wienecke, B., Heil, P., Doddridge, E. W., Sallée, J.-B., Williams, T. J., Reading, A. M., Mackintosh, A., Reese, R., Winkelmann, R., Klose, A. K., Boyd, P. W., Chown, S. L., and Robinson, S. A.: Emerging evidence of abrupt changes in the Antarctic environment, Nature, 644, 621–633, https://doi.org/10.1038/s41586-025-09349-5, 2025.

Ackley, S. F.: Pressure ridge associated microbial communities in Antarctic sea ice, Eos, Trans. Am. Geophys. Union, 66, 1278, https://doi.org/10.1029/EO066i051p01257, 1985.

Ackley, S. F. and Sullivan, C. W.: Physical controls on the development and characteristics of Antarctic sea ice biological communities - A review and synthesis, Deep-Sea Res. Part I: Oceanogr. Res. Papers, 41, 1583–1604, https://doi.org/10.1016/0967-0637(94)90062-0, 1994.

Ackley, S. F., Stammerjohn, S., Maksym, T., Smith, M., Cassano, J., Guest, P., Tison, J. L., Delille, B., Loose, B., Sedwick, P., DePace, L., Roach, L., and Parno, J.: Sea-ice production and air/ice/ocean/biogeochemistry interactions in the Ross Sea during the PIPERS 2017 autumn field campaign, Ann. Glaciol., 61, 181–195, https://doi.org/10.1017/aog.2020.31, 2020.

Alberello, A., Bennetts, L. G., Onorato, M., Vichi, M., MacHutchon, K., Eayrs, C., Ntamba, B. N., Benetazzo, A., Bergamasco, F., Nelli, F., Pattani, R., Clarke, H., Tersigni, I., and Toffoli, A.: Three-dimensional imaging of waves and floes in the marginal ice zone during a cyclone, Nat. Commun., 13, 4590, https://doi.org/10.1038/s41467-022-32036-2, 2022.

Allison, I., Brandt, R. E., and Warren, S. G.: East Antarctic sea ice: Albedo, thickness distribution, and snow cover, J. Geophys. Res.-Oceans, 98, 12417–12429, https://doi.org/10.1029/93jc00648, 1993.

Andreas, E. L. and Ackley, S. F.: On the Differences in Ablation Seasons of Arctic and Antarctic Sea Ice, J. Atmos. Sci., 39, 440–447, https://doi.org/10.1175/1520-0469(1982)039<0440:Otdias>2.0.Co;2, 1982.

Arrigo, K. R., Perovich, D. K., Pickart, R. S., Brown, Z. W., van Dijken, G. L., Lowry, K. E., Mills, M. M., Palmer, M. A., Balch, W. M., Bahr, F., Bates, N. R., Benitez-Nelson, C., Bowler, B., Brownlee, E., Ehn, J. K., Frey, K. E., Garley, R., Laney, S. R., Lubelczyk, Mathis, J., Matsuoka, A., Mitchell, B. G., Moore, G. W. K., Ortega-Retuerta, E., Pal, S., Polashenski, C. M., Reynolds, R. A., Schieber, B., Sosik, H. M., Stephens, M., and Swift, J. H.: Massive Phytoplankton Blooms Under Arctic Sea Ice, Science, 336, 1408–1408, https://doi.org/10.1126/science.1215065, 2012.

Arrigo, K. R., Brown, Z. W., Mills, M. M., Deming, J. W., and Tremblay, J.-É.: Sea ice algal biomass and physiology in the Amundsen Sea, Antarctica, Elem. Sc. Anthrop., 2, https://doi.org/10.12952/journal.elementa.000028, 2014.

Arrigo, K. R. and van Dijken, G. L.: Phytoplankton dynamics within 37 Antarctic coastal polynya systems, J. Geophys. Res.-Oceans, 108, https://doi.org/10.1029/2002jc001739, 2003.

Asplin, M. G., Galley, R., Barber, D. G., and Prinsenberg, S.: Fracture of summer perennial sea ice by ocean swell as a result of Arctic storms, J. Geophys. Res.-Oceans, 117, https://doi.org/10.1029/2011jc007221, 2012.

Asplin, M. G., Scharien, R., Else, B., Howell, S., Barber, D. G., Papakyriakou, T., and Prinsenberg, S.: Implications of fractured Arctic perennial ice cover on thermodynamic and dynamic sea ice processes, J. Geophys. Res.-Oceans, 119, 2327–2343, https://doi.org/10.1002/2013jc009557, 2014.

Auger, M., Sallée, J. B., Thompson, A. F., Pauthenet, E., and Prandi, P.: Southern Ocean Ice-Covered Eddy Properties From Satellite Altimetry, J. Geophys. Res.-Oceans, 128, https://doi.org/10.1029/2022jc019363, 2023.

Ayres, H. C., Screen, J. A., Blockley, E. W., and Bracegirdle, T. J.: The Coupled Atmosphere–Ocean Response to Antarctic Sea Ice Loss, J. Climate, 35, 4665–4685, https://doi.org/10.1175/jcli-d-21-0918.1, 2022.

Barber, D. G. and Massom, R. A.: The Role of Sea Ice in Arctic and Antarctic Polynyas, in: Polynyas: Windows to the World, edited by: Smith, W. O. and Barber, D. G., Elsevier Oceanography Series, 1–54, https://doi.org/10.1016/s0422-9894(06)74001-6, 2007.

Bateson, A. W., Feltham, D. L., Schröder, D., Hosekova, L., Ridley, J. K., and Aksenov, Y.: Impact of sea ice floe size distribution on seasonal fragmentation and melt of Arctic sea ice, The Cryosphere, 14, 403–428, https://doi.org/10.5194/tc-14-403-2020, 2020.

Bennetts, L. G., O'Farrell, S., and Uotila, P.: Brief communication: Impacts of ocean-wave-induced breakup of Antarctic sea ice via thermodynamics in a stand-alone version of the CICE sea-ice model, The Cryosphere, 11, 1035–1040, https://doi.org/10.5194/tc-11-1035-2017, 2017.

Bennetts, L. G., Shakespeare, C. J., Vreugdenhil, C. A., Foppert, A., Gayen, B., Meyer, A., Morrison, A. K., Padman, L., Phillips, H. E., Stevens, C. L., Toffoli, A., Constantinou, N. C., Cusack, J. M., Cyriac, A., Doddridge, E. W., England, M. H., Evans, D. G., Heil, P., Hogg, A. M., Holmes, R. M., Huneke, W. G. C., Jones, N. L., Keating, S. R., Kiss, A. E., Kraitzman, N., Malyarenko, A., McConnochie, C. D., Meucci, A., Montiel, F., Neme, J., Nikurashin, M., Patel, R. S., Peng, J. P., Rayson, M., Rosevear, M. G., Sohail, T., Spence, P., and Stanley, G. J.: Closing the Loops on Southern Ocean Dynamics: From the Circumpolar Current to Ice Shelves and From Bottom Mixing to Surface Waves, Rev. Geophys., 62, https://doi.org/10.1029/2022rg000781, 2024.

Bennetts, L. G. and Williams, T. D.: Water wave transmission by an array of floating discs, P. Roy. Soc. A-Math. Phy., 471, https://doi.org/10.1098/rspa.2014.0698, 2015.

Brandt, R. E., Warren, S. G., Worby, A. P., and Grenfell, T. C.: Surface Albedo of the Antarctic Sea Ice Zone, J. Climate, 18, 3606–3622, https://doi.org/10.1175/jcli3489.1, 2005.

Brouwer, J., Fraser, A. D., Murphy, D. J., Wongpan, P., Alberello, A., Kohout, A., Horvat, C., Wotherspoon, S., Massom, R. A., Cartwright, J., and Williams, G. D.: Altimetric observation of wave attenuation through the Antarctic marginal ice zone using ICESat-2, The Cryosphere, 16, 2325–2353, https://doi.org/10.5194/tc-16-2325-2022, 2022.

Casas-Prat, M., Hemer, M. A., Dodet, G., Morim, J., Wang, X. L., Mori, N., Young, I., Erikson, L., Kamranzad, B., Kumar, P., Menéndez, M., and Feng, Y.: Wind-wave climate changes and their impacts, Nature Reviews Earth & Environment, 5, 23–42, https://doi.org/10.1038/s43017-023-00502-0, 2024.

Cavalieri, D., Parkinson, C., Gloersen, P., and Zwally, H. J.: Sea ice concentrations from Nimbus-7 SMMR and DMSP SSM/I-SSMIS passive microwave data, NSIDC-0051 Version 1, Boulder, Colorado, USA, NASA National Snow and Ice Data Center Distributed Active Archive Center [data set], https://doi.org/10.5067/8GQ8LZQVL0VL, 1996.

Chai, W., Leira, B. J., Høyland, K. V., Sinsabvarodom, C., and Yu, Z.: Statistics of thickness and strength of first-year ice along the Northern Sea Route, J. Mar. Sci. Tech., 26, 331–343, https://doi.org/10.1007/s00773-020-00742-5, 2020.

Charlson, R. J., Lovelock, J. E., Andreae, M. O., and Warren, S. G.: Oceanic phytoplankton, atmospheric sulphur, cloud albedo and climate, Nature, 326, 655–661, https://doi.org/10.1038/326655a0, 1987.

Comiso, J. C., Gersten, R. A., Stock, L. V., Turner, J., Perez, G. J., and Cho, K.: Positive Trend in the Antarctic Sea Ice Cover and Associated Changes in Surface Temperature, J. Climate, 30, 2251–2267, https://doi.org/10.1175/jcli-d-16-0408.1, 2017a.

Comiso, J. C., Meier, W. N., and Gersten, R.: Variability and trends in the Arctic Sea ice cover: Results from different techniques, J. Geophys. Res.-Oceans, 122, 6883–6900, https://doi.org/10.1002/2017jc012768, 2017b.

Comiso, J. C. and Steffen, K.: Studies of Antarctic sea ice concentrations from satellite data and their applications, J. Geophys. Res.-Oceans, 106, 31361–31385, https://doi.org/10.1029/2001jc000823, 2001.

Comiso, J. C., Grenfell, T. C., Lange, M., Lohanick, A. W., Moore, R. K., and Wadhams, P.: Microwave remote sensing of the Southern Ocean ice cover, in: Microwave Remote Sensing of Sea Ice, edited by Carsey, F. D., Geophysical Monograph Series, American Geophysical Union, Washington DC, USA, 243–259, https://doi.org/10.1029/GM068p0243, 1992.

Corkill, M., Moreau, S., Janssens, J., Fraser, A. D., Heil, P., Tison, J. L., Cougnon, E. A., Genovese, C., Kimura, N., Meiners, K. M., Wongpan, P., and Lannuzel, D.: Physical and Biogeochemical Properties of Rotten East Antarctic Summer Sea Ice, J. Geophys. Res.-Oceans, 128, https://doi.org/10.1029/2022jc018875, 2023.

Curry, J. A., Schramm, J. L., and Ebert, E. E.: Sea Ice-Albedo Climate Feedback Mechanism, J. Climate, 8, 240–247, https://doi.org/10.1175/1520-0442(1995)008<0240:Siacfm>2.0.Co;2, 1995.

Curry, J. A., Schramm, J. L., Perovich, D. K., and Pinto, J. O.: Applications of SHEBA/FIRE data to evaluation of snow/ice albedo parameterizations, J. Geophys. Res. Atmos., 106, 15345–15355, https://doi.org/10.1029/2000jd900311, 2001.

Dai, M., Shen, H. H., Hopkins, M. A., and Ackley, S. F.: Wave rafting and the equilibrium pancake ice cover thickness, J. Geophys. Res.-Oceans, 109, https://doi.org/10.1029/2003jc002192, 2004.

Dalman, L. A., Meiners, K. M., Thomas, D. N., Deman, F., Bestley, S., Moreau, S., Arrigo, K. R., Campbell, K., Corkill, M., Cozzi, S., Delille, B., Fransson, A., Fraser, A. D., Henley, S. F., Janssens, J., Lannuzel, D., Munro, D. R., Nomura, D., Norman, L., Papadimitriou, S., Schallenberg, C., Tison, J. L., Vancoppenolle, M., van der Merwe, P., and Fripiat, F.: Observation-Based Estimate of Net Community Production in Antarctic Sea Ice, Geophys. Res. Lett., 52, https://doi.org/10.1029/2024gl113717, 2025.

Day, N. S., Bennetts, L. G., O'Farrell, S. P., Alberello, A., and Montiel, F.: Analysis of the Antarctic Marginal Ice Zone Based on Unsupervised Classification of Standalone Sea Ice Model Data, J. Geophys. Res.-Oceans, 129, https://doi.org/10.1029/2024jc020953, 2024.

Diamond, R., Schroeder, D., Sime, L. C., Ridley, J., and Feltham, D.: The significance of the melt-pond scheme in a CMIP6 Global Climate Mode. J. Climate, 37, 249-268, https://doi.org/10.1175/JCLI-D-22-0902.1, 2023.

Drinkwater, M. R. and Liu, X.: Seasonal to interannual variability in Antarctic sea-ice surface melt, IEEE Trans. Geosc. Rem. Sens., 38, 1827–1842, https://doi.org/10.1109/36.851767, 2000.

Dubey, U., Willmes, S., and Heinemann, G.: Southern Ocean sea-ice leads: first insights into regional lead patterns, seasonality, and trends, 2003–2023, The Cryosphere, 19, 3535–3552, https://doi.org/10.5194/tc-19-3535-2025, 2025.

Ducklow, H., Fraser, W., Meredith, M., Stammerjohn, S., Doney, S., Martinson, D., Sailley, S., Schofield, O., Steinberg, D., Venables, H., and Amsler, C.: West Antarctic Peninsula: An Ice-Dependent Coastal Marine Ecosystem in Transition, Oceanog., 26, 190–203, https://doi.org/10.5670/oceanog.2013.62, 2013.

Eayrs, C., Holland, D., Francis, D., Wagner, T., Kumar, R., and Li, X.: Understanding the Seasonal Cycle of Antarctic Sea Ice Extent in the Context of Longer-Term Variability, Rev. Geophys., 57, 1037–1064, https://doi.org/10.1029/2018rg000631, 2019.

Ebert, E. E. and Curry, J. A.: An intermediate one-dimensional thermodynamic sea ice model for investigating ice-atmosphere interactions, J. Geophys. Res.-Oceans, 98, 10085–10109, https://doi.org/10.1029/93jc00656, 1993.

Eicken, H., Ackley, S. F., Richter-Menge, J. A., and Lange, M. A.: Is the strength of sea ice related to its chlorophyll content?, Polar Biol., 11, https://doi.org/10.1007/bf00239027, 1991.

Eicken, H., Fischer, H., and Lemke, P.: Effects of the snow cover on Antarctic sea ice and potential modulation of its response to climate change, Ann. Glaciol., 21, 369–376, https://doi.org/10.3189/s0260305500016086, 1995.

Eicken, H., Lange, M. A., and Wadhams, P.: Characteristics and distribution patterns of snow and meteoric ice in the Weddell Sea and their contribution to the mass balance of sea ice, Ann. Geophys., 12, 80–93, https://doi.org/10.1007/s00585-994-0080-x, 1994.

England, M., Polvani, L., and Sun, L.: Contrasting the Antarctic and Arctic Atmospheric Responses to Projected Sea Ice Loss in the Late Twenty-First Century, J. Climate, 31, 6353–6370, https://doi.org/10.1175/jcli-d-17-0666.1, 2018.

England, M. R., Polvani, L. M., Sun, L., and Deser, C.: Tropical climate responses to projected Arctic and Antarctic sea-ice loss, Nat. Geosci., 13, 275–281, https://doi.org/10.1038/s41561-020-0546-9, 2020.

Enomoto, H. and Ohmura, A.: The influences of atmospheric half-yearly cycle on the sea ice extent in the Antarctic, J. Geophys. Res.-Oceans, 95, 9497–9511, https://doi.org/10.1029/JC095iC06p09497, 1990.

Fang, Y., Wu, T., Hu, A., and Chu, M.: A modified thermodynamic sea ice model and its application, Ocean Model., 178, https://doi.org/10.1016/j.ocemod.2022.102096, 2022.

Fetterer, F. and Untersteiner, N.: Observations of melt ponds on Arctic sea ice, J. Geophys. Res.-Oceans, 103, 24821–24835, https://doi.org/10.1029/98jc02034, 1998.

Fitzpatrick, M. F. and Warren, S. G.: Transmission of Solar Radiation by Clouds over Snow and Ice Surfaces. Part II: Cloud Optical Depth and Shortwave Radiative Forcing from Pyranometer Measurements in the Southern Ocean, J. Climate, 18, 4637–4648, https://doi.org/10.1175/jcli3562.1, 2005.

Fitzpatrick, M. F. and Warren, S. G.: The Relative Importance of Clouds and Sea Ice for the Solar Energy Budget of the Southern Ocean, J. Climate, 20, 941–954, https://doi.org/10.1175/jcli4040.1, 2007.

Flocco, D., Feltham, D. L., and Turner, A. K.: Incorporation of a physically based melt pond scheme into the sea ice component of a climate model, J. Geophys. Res.-Oceans, 115, https://doi.org/10.1029/2009jc005568, 2010.

Fraser, A. D., Wongpan, P., Langhorne, P. J., Klekociuk, A. R., Kusahara, K., Lannuzel, D., Massom, R. A., Meiners, K. M., Swadling, K. M., Atwater, D. P., Brett, G. M., Corkill,

M., Dalman, L. A., Fiddes, S., Granata, A., Gugliemo, L., Heil, P., Leonard, G. H., Mahoney, A. R., McMinn, A., van der Merwe, P., Weldrick C. K., and Wienecke, B.: Antarctic landfast sea ice: A review of its physics, biogeochemistry and ecology, Rev. Geophys., 61, e2022RG000770, https://doi.org/10.1029/2022RG000770, 2023.

Fraser, A. D., Day, N., Wang, Z., Bennetts, L. G., Liu, Q., O'Farrell, S., Coleman, R., Voermans, J., Xu, S., Zhu, W., Auger, M., Massom, R. A., Wongpan, P., Craw, L., Brouwer, J., Toyota, T., Heil, P., and Horvat, C.: Revealing the Antarctic marginal ice zone: a decade-long wave-in-ice climatology, Nat. Commun., in press, 2026.

Frölicher, T. L., Sarmiento, J. L., Paynter, D. J., Dunne, J. P., Krasting, J. P., and Winton, M.: Dominance of the Southern Ocean in Anthropogenic Carbon and Heat Uptake in CMIP5 Models, J. Climate, 28, 862–886, https://doi.org/10.1175/jcli-d-14-00117.1, 2015.

Garrison, D. L., Jeffries, M. O., Gibson, A., Coale, S. L., Neenan, D., Fritsen, C., Okolodkov, Y. B., and Gowing, M. M.: Development of sea ice microbial communities during autumn ice formation in the Ross Sea, Mar. Ecol. Prog. Ser., 259, 1–15, https://doi.org/10.3354/meps259001, 2003.

Gebhardt, C., Bidlot, J.-R., Gemmrich, J., Lehner, S., Pleskachevsky, A., and Rosenthal, W.: Wave observation in the marginal ice zone with the TerraSAR-X satellite, Ocean Dynam., 66, 839–852, https://doi.org/10.1007/s10236-016-0957-8, 2016.

Godfred-Spenning, C. R. and Simmonds, I.: An Analysis of Antarctic Sea-Ice and Extratropical Cyclone Associations, Int. J. Climatol., 16, 1315–1332, https://doi.org/10.1002/(sici)1097-0088(199612)16:12<1315::Aid-joc92>3.0.Co;2-m, 1996.

Golden, K. M., Ackley, S. F., and Lytle, V. I.: The Percolation Phase Transition in Sea Ice, Science, 282, 2238–2241, https://doi.org/10.1126/science.282.5397.2238, 1998.

Goosse, H., Allende Contador, S., Bitz, C. M., Blanchard-Wrigglesworth, E., Eayrs, C., Fichefet, T., Himmich, K., Huot, P.-V., Klein, F., Marchi, S., Massonnet, F., Mezzina, B., Pelletier, C., Roach, L., Vancoppenolle, M., and van Lipzig, N. P. M.: Modulation of the seasonal cycle of the Antarctic sea ice extent by sea ice processes and feedbacks with the ocean and the atmosphere, The Cryosphere, 17, 407–425, https://doi.org/10.5194/tc-17-407-2023, 2023.

Goosse, H., Kay, J. E., Armour, K. C., Bodas-Salcedo, A., Chepfer, H., Docquier, D., Jonko, A., Kushner, P. J., Lecomte, O., Massonnet, F., Park, H. S., Pithan, F., Svensson, G., and Vancoppenolle, M.: Quantifying climate feedbacks in polar regions, Nat. Commun., 9, 1919, https://doi.org/10.1038/s41467-018-04173-0, 2018.

Gordon, A. L.: Seasonality of Southern Ocean sea ice, J. Geophys. Res. Oceans, 86, 4193–4197, https://doi.org/10.1029/JC086iC05p04193, 1981.

Gordon, A. L. and Taylor, H. W.: Seasonal change of Antarctic sea ice cover, Science, 187, 346–347, https://doi.org/10.1126/science.187.4174.346, 1975.

Grenfell, T. C. and Maykut, G. A.: The Optical Properties of Ice and Snow in the Arctic Basin, J. Glaciol., 18, 445–463, https://doi.org/10.3189/s0022143000021122, 1977.

Grenfell, T. C. and Perovich, D. K.: Seasonal and spatial evolution of albedo in a snow-ice-land-ocean environment, J. Geophys. Res.-Oceans, 109, https://doi.org/10.1029/2003jc001866, 2004.

Hague, M. and Vichi, M.: Southern Ocean Biogeochemical Argo detect under-ice phytoplankton growth before sea ice retreat, Biogeosciences, 18, 25–38, https://doi.org/10.5194/bg-18-25-2021, 2021.

Hartmann, D. L.: Global Physical Climatology (Second Edition), Elsevier, Boston, ISBN 978-0-12-328531-7, 2016.

Hauck, J., Völker, C., Wolf-Gladrow, D. A., Laufkötter, C., Vogt, M., Aumont, O., Bopp, L., Buitenhuis, E. T., Doney, S. C., Dunne, J., Gruber, N., Hashioka, T., John, J., Le Quéré, C., Lima, I. D., Nakano, H., Séférian, R., and Totterd, I.: On the Southern Ocean CO_2 uptake and the role of the biological carbon pump in the 21st century, Global Biogeochem. Cy., 29, 1451–1470, https://doi.org/10.1002/2015GB005140, 2015.

Haumann, F. A., Gruber, N., Munnich, M., Frenger, I., and Kern, S.: Sea-ice transport driving Southern Ocean salinity and its recent trends, Nature, 537, 89–92, https://doi.org/10.1038/nature19101, 2016.

Henley, S. F., Cavan, E. L., Fawcett, S. E., Kerr, R., Monteiro, T., Sherrell, R. M., Bowie, A. R., Boyd, P. W., Barnes, D. K. A, Schloss, I. R., Marshall, T., Flynn, R., and Smith, S.: Changing biogeochemistry of the Southern Ocean and its ecosystem implications, Frontiers in Marine Science, 7, https://doi.org/10.3389/fmars.2020.00581, 2020.

Herman, A. and Bradtke, K.: Fetch-Limited, Strongly Forced Wind Waves in Waters With Frazil and Grease Ice – Spectral Modeling and Satellite Observations in an Antarctic Coastal Polynya, J. Geophys. Res.-Oceans, 129, https://doi.org/10.1029/2023jc020452, 2024.

Hobbs, W., Spence, P., Meyer, A., Schroeter, S., Fraser, A. D., Reid, P., Tian, T. R., Wang, Z., Liniger, G., Doddridge, E. W., and Boyd, P. W.: Observational Evidence for a Regime Shift in Summer Antarctic Sea Ice, J. Climate, 37, 2263–2275, https://doi.org/10.1175/jcli-d-23-0479.1, 2024.

Holland, M. M. and Bitz, C. M.: Polar amplification of climate change in coupled models, Clim. Dynam., 21, 221–232, https://doi.org/10.1007/s00382-003-0332-6, 2003.

Horvat, C.: Floes, the marginal ice zone and coupled wave-sea-ice feedbacks, Phil. Trans. A. Math. Phys. Eng. Sci., 380, 20210252, https://doi.org/10.1098/rsta.2021.0252, 2022.

Horvat, C. and Tziperman, E.: Understanding Melting due to Ocean Eddy Heat Fluxes at the Edge of Sea-Ice Floes, Geophys. Res. Lett., 45, 9721–9730, https://doi.org/10.1029/2018gl079363, 2018.

Horvat, C., Bisson, K., Seabrook, S., Cristi, A., and Matthes, L. C.: Evidence of phytoplankton blooms under Antarctic sea ice, Front. Mar. Sci. 9, 942799, https://doi.org/10.3389/fmars.2022.942799, 2022.

Inoue, J., Kikuchi, T., and Perovich, D. K.: Effect of heat transmission through melt ponds and ice on melting during summer in the Arctic Ocean, J. Geophys. Res.-Oceans, 113, https://doi.org/10.1029/2007jc004182, 2008.

Intergovernmental Panel on Climate Change (IPCC): Observations: Atmosphere and Surface, in: Climate Change 2013 – The Physical Science Basis: Working Group I Contribution to the Fifth Assessment Report of the Intergovernmental Panel

on Climate Change, 159-254, Cambridge University Press, https://doi.org/10.1017/CBO9781107415324, 2014.

Ishida, K. and Ohshima, K. I.: Ice-band characteristics of the Antarctic seasonal ice zone observed using MOS MESSR images, Atmos.-Ocean, 47, 169–183, https://doi.org/10.3137/oc300.2009, 2009.

Ivanova, N., Pedersen, L. T., Tonboe, R. T., Kern, S., Heygster, G., Lavergne, T., Sørensen, A., Saldo, R., Dybkjær, G., Brucker, L., and Shokr, M.: Inter-comparison and evaluation of sea ice algorithms: towards further identification of challenges and optimal approach using passive microwave observations, The Cryosphere, 9, 1797–1817, https://doi.org/10.5194/tc-9-1797-2015, 2015.

Kacimi, S. and Kwok, R.: The Antarctic sea ice cover from ICESat-2 and CryoSat-2: freeboard, snow depth, and ice thickness, The Cryosphere, 14, 4453–4474, https://doi.org/10.5194/tc-14-4453-2020, 2020.

Kashiwase, H., Ohshima, K. I., Nihashi, S., and Eicken, H.: Evidence for ice-ocean albedo feedback in the Arctic Ocean shifting to a seasonal ice zone, Sci. Rep., 7, 8170, https://doi.org/10.1038/s41598-017-08467-z, 2017.

Kennicutt, M. C., Chown, S. L., Cassano, J. J., Liggett, D., Peck, L. S., Massom, R., Rintoul, S. R., Storey, J., Vaughan, D. G., Wilson, T. J., Allison, I., Ayton, J., Badhe, R., Baeseman, J., Barrett, P. J., Bell, R. E., Bertler, N., Bo, S., Brandt, A., Bromwich, D., Cary, S. C., Clark, M. S., Convey, P., Costa, E. S., Cowan, D., Deconto, R., Dunbar, R., Elfring, C., Escutia, C., Francis, J., Fricker, H. A., Fukuchi, M., Gilbert, N., Gutt, J., Havermans, C., Hik, D., Hosie, G., Jones, C., Kim, Y. D., Le Maho, Y., Lee, S. H., Leppe, M., Leitchenkov, G., Li, X., Lipenkov, V., Lochte, K., López-Martínez, J., Lüdecke, C., Lyons, W., Marenssi, S., Miller, H., Morozova, P., Naish, T., Nayak, S., Ravindra, R., Retamales, J., Ricci, C. A., Rogan-Finnemore, M., Ropert-Coudert, Y., Samah, A. A., Sanson, L., Scambos, T., Schloss, I. R., Shiraishi, K., Siegert, M. J., Simões, J. C., Storey, B., Sparrow, M. D., Wall, D. H., Walsh, J. C., Wilson, G., Winther, J. G., Xavier, J. C., Yang, H., and Sutherland, W. J.: A roadmap for Antarctic and Southern Ocean science for the next two decades and beyond, Antarct. Sci., 27, 3–18, https://doi.org/10.1017/s0954102014000674, 2014.

Kimura, N., Onomura, T., and Kikuchi, T.: Processes governing seasonal and interannual change of the Antarctic sea-ice area, J. Oceanogr., 79, 109–121, https://doi.org/10.1007/s10872-022-00669-y, 2022.

Kohout, A. L., Williams, M. J., Dean, S. M., and Meylan, M. H.: Storm-induced sea-ice breakup and the implications for ice extent, Nature, 509, 604–607, https://doi.org/10.1038/nature13262, 2014.

Kohout, A. L., Williams, M. J. M., Toyota, T., Lieser, J., and Hutchings, J.: In situ observations of wave-induced sea ice breakup, Deep-Sea Res. Part B: Top. St. Oceanog., 131, 22–27, https://doi.org/10.1016/j.dsr2.2015.06.010, 2016.

Kottmeier, S. T. and Sullivan, C. W.: Bacterial biomass and production in pack ice of Antarctic marginal ice edge zones, Deep-Sea Res. Part A. Oceanogr. Res. Papers, 37, 1311–1330, https://doi.org/10.1016/0198-0149(90)90045-w, 1990.

Light, B., Perovich, D. K., Webster, M. A., Polashenski, C., and Dadic, R.: Optical properties of melting first-year Arctic sea ice, J. Geophys. Res.-Oceans, 120, 7657–7675, https://doi.org/10.1002/2015jc011163, 2015.

Light, B., Smith, M. M., Perovich, D. K., Webster, M. A., Holland, M. M., Linhardt, F., Raphael, I. A., Clemens-Sewall, D., Macfarlane, A. R., Anhaus, P., and Bailey, D. A.: Arctic sea ice albedo: Spectral composition, spatial heterogeneity, and temporal evolution observed during the MOSAiC drift, Elem.: Sc. Anthrop., 10, https://doi.org/10.1525/elementa.2021.000103, 2022.

Liu, A. K. and Mollo-Christensen, E.: Wave Propagation in a Solid Ice Pack, J. Phys. Oceanogr., 18, 1702–1712, https://doi.org/10.1175/1520-0485(1988)018<1702:Wpiasi>2.0.Co;2, 1988.

Liu, J., Li, R., Li, S., Meucci, A., and Young, I. R.: Increasing wave power due to global climate change and intensification of Antarctic Oscillation, Applied Energy, 358, 122572, https://doi.org/10.1016/j.apenergy.2023.122572, 2024.

Louw, S. D. V., Walker, D. R., and Fawcett, S. E.: Factors influencing sea-ice algae abundance, community composition, and distribution in the marginal ice zone of the Southern Ocean during winter, Deep-Sea Res. Part A. Oceanogr. Res. Papers, 185, https://doi.org/10.1016/j.dsr.2022.103805, 2022.

Lubin, D. and Massom, R. A.: Polar Remote Sensing. Volume 1: Atmosphere and Oceans. Praxis/Springer, Chichester, UK, and Berlin, Germany, 756 pp., https://doi.org/10.1007/3-540-30785-0, 2006.

Lüthje, M., Feltham, D. L., Taylor, P. D., and Worster, M. G.: Modeling the summertime evolution of sea-ice melt ponds, J. Geophys. Res.-Oceans, 111, https://doi.org/10.1029/2004jc002818, 2006.

Maksym, T.: Arctic and Antarctic Sea Ice Change: Contrasts, Commonalities, and Causes, Ann. Rev. Mar. Sci., 11, 187–213, https://doi.org/10.1146/annurev-marine-010816-060610, 2019.

Maksym, T. and Markus, T.: Antarctic sea ice thickness and snow-to-ice conversion from atmospheric reanalysis and passive microwave snow depth, J. Geophys. Res.-Oceans, 113, https://doi.org/10.1029/2006jc004085, 2008.

Maksym, T., Stammerjohn, S., Ackley, S., and Massom, R.: Antarctic Sea Ice – A Polar Opposite?, Oceanogr., 25, 140–151, https://doi.org/10.5670/oceanog.2012.88, 2012.

Mallet, M. D., Miljevic, B., Humphries, R. S., Mace, G, Alexander, S. P., Protat, A., Chambers, S., Cravigan, L., DeMott, P. J., Fiddes, S., Harnwell, J., Keywood, M. D., McFarquhar, G. M., McRobert, I., Moore, K. A., Mynard, C., Godday Osuagwu, C., Ristovski, Z., Selleck, P., Taylor, S., Ward, J., and Williams, A.: Biological enhancement of cloud droplet concentrations observed off East Antarctica, npj Clim. Atmos. Sci., 8, 113, https://doi.org/10.1038/s41612-025-00990-5, 2025.

Manabe, S. and Stouffer, R. J.: Sensitivity of a global climate model to an increase of CO_2 concentration in the atmosphere, J. Geophys. Res.-Oceans, 85, 5529–5554, https://doi.org/10.1029/JC085iC10p05529, 1980.

Martin, S., Kauffman, P., and Parkinson, C.: The movement and decay of ice edge bands in the winter Bering Sea, J. Geophys. Res.-Oceans, 88, 2803–2812, https://doi.org/10.1029/JC088iC05p02803, 1983.

Maslanik, J. A., Fowler, C., Stroeve, J., Drobot, S., Zwally, J., Yi, D., and Emery, W.: A younger, thinner Arctic ice cover: Increased potential for rapid, extensive sea-ice loss, Geophys. Res. Lett., 34, https://doi.org/10.1029/2007gl032043, 2007.

Massom, R. A.: Satellite Remote Sensing of Polar Regions: Applications, Limitations and Data Availability, Belhaven Press, London (UK) and Lewis Publishers, Boca Raton (USA), 307 pp., ISBN O-87372-607-8, 1991.

Massom, R. A. and Stammerjohn, S. E.: Antarctic sea ice change and variability – Physical and ecological implications, Polar Sci., 4, 149–186, https://doi.org/10.1016/j.polar.2010.05.001, 2010.

Massom, R. A., Drinkwater, M. R., and Haas, C.: Winter snow cover on sea ice in the Weddell Sea, J. Geophys. Res.-Oceans, 102, 1101–1117, https://doi.org/10.1029/96jc02992, 1997.

Massom, R. A., Lytle, V. I., Worby, A. P., and Allison, I.: Winter snow cover variability on East Antarctic sea ice, J. Geophys. Res.-Oceans, 103, 24837–24855, https://doi.org/10.1029/98jc01617, 1998.

Massom, R. A., Comiso, J. C., Worby, A. P., Lytle, V. I., and Stock, L.: Regional Classes of Sea Ice Cover in the East Antarctic Pack Observed from Satellite and In Situ Data during a Winter Time Period, Remote Sens. Environ., 68, 61–76, https://doi.org/10.1016/s0034-4257(98)00100-x, 1999.

Massom, R. A., Eicken, H., Hass, C., Jeffries, M. O., Drinkwater, M. R., Sturm, M., Worby, A. P., Wu, X., Lytle, V. I., Ushio, S., Morris, K., Reid, P. A., Warren, S. G., and Allison, I.: Snow on Antarctic sea ice, Rev. Geophys., 39, 413–445, https://doi.org/10.1029/2000rg000085, 2001.

Massom, R. A., Jacka, K., Pook, M. J., Fowler, C., Adams, N., and Bindoff, N.: An anomalous late-season change in the regional sea ice regime in the vicinity of the Mertz Glacier Polynya, East Antarctica, J. Geophys. Res.-Oceans, 108, https://doi.org/10.1029/2002jc001354, 2003.

Massom, R. A., Stammerjohn, S. E., Smith, R. C., Pook, M. J., Iannuzzi, R. A., Adams, N., Martinson, D. G., Vernet, M., Fraser, W. R., Quetin, L. B., Ross, R. M., Massom, Y., and Krouse, H. R.: Extreme Anomalous Atmospheric Circulation in the West Antarctic Peninsula Region in Austral Spring and Summer 2001/02, and Its Profound Impact on Sea Ice and Biota, J. Climate, 19, 3544–3571, https://doi.org/10.1175/jcli3805.1, 2006.

Massom, R. A., Stammerjohn, S. E., Lefebvre, W., Harangozo, S. A., Adams, N., Scambos, T. A., Pook, M. J., and Fowler, C.: West Antarctic Peninsula sea ice in 2005: Extreme ice compaction and ice edge retreat due to strong anomaly with respect to climate, J. Geophys. Res.-Oceans, 113, https://doi.org/10.1029/2007jc004239, 2008.

Massom, R. A., Reid, P., Stammerjohn, S., Raymond, B., Fraser, A., and Ushio, S.: Change and variability in East Antarctic sea ice seasonality, 1979/80–2009/10, PLoS One, 8, e64756, https://doi.org/10.1371/journal.pone.0064756, 2013.

Massom, R. A., Scambos, T. A., Bennetts, L. G., Reid, P., Squire, V. A., and Stammerjohn, S. E.: Antarctic ice shelf disintegration triggered by sea ice loss and ocean swell, Nature, 558, 383–389, https://doi.org/10.1038/s41586-018-0212-1, 2018.

Maykut, G. A. and Perovich, D. K.: The role of shortwave radiation in the summer decay of a sea ice cover, J. Geophys. Res.-Oceans, 92, 7032–7044, https://doi.org/10.1029/JC092iC07p07032, 1987.

Meehl, G. A. and Washington, W. M.: CO_2 climate sensitivity and snow-sea-ice albedo parameterization in an atmospheric GCM coupled to a mixed-layer ocean model, Climatic Change, 16, 283–306, https://doi.org/10.1007/bf00144505, 1990.

Mellor, M.: Mechanical Behavior of Sea Ice, in: The Geophysics of Sea Ice, edited by: Untersteiner, N., Springer, Boston, USA, 165–281, https://doi.org/10.1007/978-1-4899-5352-0_3, 1986.

Meredith, M., Sommerkorn, M., Cassotta, S., Derksen, C., Ekaykin, A., Hollowed, A., Kofinas, G., Mackintosh, A., Melbourne-Thomas, J., Muelbert, M. M. C., Ottersen, G., Pritchard, H., and Schuur, E. A. G.: Polar Regions. In: The Ocean and Cryosphere in a Changing Climate, Cambridge University Press, Cambridge UK, 203–320, https://doi.org/10.1017/9781009157964.005, 2022.

Meredith, M. P. and Brandon, M. A.: Oceanography and sea ice in the Southern Ocean, in: Sea Ice, edited by: Thomas, D. N., Wiley-Blackwell, Oxford (UK), 216–238, https://doi.org/10.1002/9781118778371.ch8, 2017.

Morim, J., Hemer, M., Wang, X. L., Cartwright, N., Trenham, C., Semedo, A., Young, I., Bricheno, L., Camus, P., Casas-Prat, M., Erikson, L., Mentaschi, L., Mori, N., Shimura, T., Timmermans, B., Aarnes, O., Breivik, Ø., Behrens, A., Dobrynin, M., Menendez, M., Staneva, J., Wehner, M., Wolf, J., Kamranzad, B., Webb, A., Stopa, J., and Andutta, F.: Robustness and uncertainties in global multivariate wind-wave climate projections, Nat. Clim. Change, 9, 711–718, https://doi.org/10.1038/s41558-019-0542-5, 2019.

Morris, K., Jeffries, M., and Li, S.: Sea Ice Characteristics and Seasonal Variability of ERS-1 SAR Backscatter in the Bellingshausen Sea, in Antarctic Sea Ice Physical Processes, Interactions and Variability, edited by: Jeffries, M. O., American Geophysical Union, Washington DC, USA, 213–242, https://doi.org/10.1029/AR074, 1998.

Muchow, M., Schmitt, A. U., and Kaleschke, L.: A lead-width distribution for Antarctic sea ice: a case study for the Weddell Sea with high-resolution Sentinel-2 images, The Cryosphere, 15, 4527–4537, https://doi.org/10.5194/tc-15-4527-2021, 2021.

National Academies of Sciences, Engineering, and Medicine (NAS): Antarctic Sea Ice Variability in the Southern Ocean-Climate System: Proceedings of a Workshop, The National Academies Press, Washington DC, USA, https://doi.org/10.17226/24696, 2017.

Nelli, F., Bennetts, Luke G., Skene, David M., and Toffoli, A.: Water wave transmission and energy dissipation by a floating plate in the presence of overwash, J. Fluid Mech., 889, https://doi.org/10.1017/jfm.2020.75, 2020.

Nicolaus, M., Gerland, S., Hudson, S. R., Hanson, S., Haapala, J., and Perovich, D. K.: Seasonality of spectral albedo and transmittance as observed in the Arctic Transpolar Drift in 2007, J. Geophys. Res.-Oceans, 115, https://doi.org/10.1029/2009jc006074, 2010.

Nicolaus, M., Katlein, C., Maslanik, J., and Hendricks, S.: Changes in Arctic sea ice result in increasing light transmittance and absorption, Geophys. Res. Lett., 39, https://doi.org/10.1029/2012gl053738, 2012.

Nihashi, S. and Cavalieri, D. J.: Observational evidence of a hemispheric-wide ice–ocean albedo feedback effect on Antarctic sea-ice decay, J. Geophys. Res.-Oceans, 111, https://doi.org/10.1029/2005jc003447, 2006.

Nihashi, S. and Ohshima, K. I.: Relationship between ice decay and solar heating through open water in the Antarctic sea ice zone, J. Geophys. Res.-Oceans, 106, 16767–16782, https://doi.org/10.1029/2000jc000399, 2001.

Nissen, C., Lovenduski, N. S., Brooks, C. M., Hoppema, M., Timmermann, R., and Hauck, J.: Severe 21st-century ocean acidification in Antarctic Marine Protected Areas, Nat. Comm., 15, 259, https://doi.org/10.1038/s41467-023-44438-x, 2024.

Nose, T., Katsuno, T., Waseda, T., Ushio, S., Rabault, J., Kodaira, T., and Voermans, J.: Observation of wave propagation over 1000 km into Antarctica winter pack ice, Coastal Eng. J., 66, 115–131, https://doi.org/10.1080/21664250.2023.2283243, 2023.

Notz, D. and Bitz, C. M.: Sea ice in Earth system models. In: Sea Ice, edited by: Thomas, D. N., Wiley-Blackwell, Oxford, UK, 304–325, https://doi.org/10.1002/9781118778371.ch12, 2017.

Ohshima, K. I. and Nihashi, S.: A Simplified Ice–Ocean Coupled Model for the Antarctic Ice Melt Season, J. Phys. Oceanogr., 35, 188–201, https://doi.org/10.1175/jpo-2675.1, 2005.

Parkinson, C. L.: Global Sea Ice Coverage from Satellite Data: Annual Cycle and 35-Yr Trends, J. Climate, 27, 9377–9382, https://doi.org/10.1175/jcli-d-14-00605.1, 2014.

Parkinson, C. L.: A 40-y record reveals gradual Antarctic sea ice increases followed by decreases at rates far exceeding the rates seen in the Arctic, P. Natl. Acad. Sci. USA, 116, 14414–14423, https://doi.org/10.1073/pnas.1906556116, 2019.

Passerotti, G., Bennetts, L. G., von Bock und Polach, F., Alberello, A., Puolakka, O., Dolatshah, A., Monbaliu, J., and Toffoli, A.: Interactions between Irregular Wave Fields and Sea Ice: A Physical Model for Wave Attenuation and Ice Breakup in an Ice Tank, J. Phys. Oceanogr., 52, 1431–1446, https://doi.org/10.1175/jpo-d-21-0238.1, 2022.

Perovich, D. K.: The optical properties of sea ice, CRREL Monograph 96-1, US Army Corps of Engineers, Cold Regions Research and Engineering Laboratory, Hanover, USA, 25 pp., https://apps.dtic.mil/sti/tr/pdf/ADA310586.pdf (last access: 15 May 2025), 1996.

Perovich, D. K.: On the aggregate-scale partitioning of solar radiation in Arctic sea ice during the Surface Heat Budget of the Arctic Ocean (SHEBA) field experiment, J. Geophys. Res.-Oceans, 110, https://doi.org/10.1029/2004jc002512, 2005.

Perovich, D. K. and Richter-Menge, J. A.: Loss of sea ice in the Arctic, Annu. Rev. Mar. Sci., 1, 417–441, https://doi.org/10.1146/annurev.marine.010908.163805, 2009.

Perovich, D. K. and Jones, K. F.: The seasonal evolution of sea ice floe size distribution, J. Geophys. Res.-Oceans, 119, 8767–8777, https://doi.org/10.1002/2014jc010136, 2014.

Perovich, D. K., Grenfell, T. C., Richter-Menge, J. A., Light, B., Tucker, W. B., and Eicken, H.: Thin and thinner: Sea ice mass balance measurements during SHEBA, J. Geophys. Res.-Oceans, 108, https://doi.org/10.1029/2001jc001079, 2003.

Perovich, D. K., Richter-Menge, J. A., Jones, K. F., and Light, B.: Sunlight, water, and ice: Extreme Arctic sea ice melt during the summer of 2007, Geophys. Res. Lett., 35, https://doi.org/10.1029/2008gl034007, 2008.

Perovich, D. K., Grenfell, T. C., Light, B., Elder, B. C., Harbeck, J., Polashenski, C., Tucker, W. B., and Stelmach, C.: Transpolar observations of the morphological properties of Arctic sea ice, J. Geophys. Res.-Oceans, 114, https://doi.org/10.1029/2008jc004892, 2009.

Petrich, C., Eicken, H., Polashenski, C. M., Sturm, M., Harbeck, J. P., Perovich, D. K., and Finnegan, D. C.: Snow dunes: A controlling factor of melt pond distribution on Arctic sea ice, J. Geophys. Res.-Oceans, 117, https://doi.org/10.1029/2012jc008192, 2012.

Pitt, J. P. A., Bennetts, L. G., Meylan, M. H., Massom, R. A., and Toffoli, A.: Model Predictions of Wave Overwash Extent Into the Marginal Ice Zone, J. Geophys. Res.-Oceans, 127, https://doi.org/10.1029/2022jc018707, 2022.

Reid, P.: Calculation of Antarctic sea ice melt rate enhancements for "The influence of ocean waves on Antarctic sea-ice albedo and seasonal melting, and potential coupled physical and biological feedbacks", Zenodo [code and data set], https://doi.org/10.5281/zenodo.18995070, 2026.

Reid, P. and Massom, R.: Successive Antarctic sea ice extent records during 2012, 2013, and 2014, B. Am. Meteorol. Soc., 96, S163–S164, 2015.

Reid, P., Stammerjohn, S., Massom, R. A., Barreira, S., Scambos, T., and Lieser, J. L.: Sea-ice extent, concentration, and seasonality, in: State of the Climate in 2023, B. Am. Meteorol. Soc., 105, S331–S370, https://doi.org/10.1175/bams-d-24-0099.1, 2024.

Reid, P., Stammerjohn, S., Massom, R. A., Barreira, S., Scambos, T., and Lieser, J. L.: Sea-ice extent, concentration, and seasonality, in: State of the Climate in 2024, B. Am. Meteorol. Soc., 108, S378–S381, https://doi.org/10.1175/BAMS-D-25-0087.1, 2025.

Riihelä, A., Bright, R. M., and Anttila, K.: Recent strengthening of snow and ice albedo feedback driven by Antarctic sea-ice loss, Nat. Geosci., 14, 832–836, https://doi.org/10.1038/s41561-021-00841-x, 2021.

Roach, L. A., Bitz, C. M., Horvat, C., and Dean, S. M.: Advances in Modeling Interactions Between Sea Ice and Ocean Surface Waves, J. Adv. Model. Earth Syst., 11, 4167–4181, https://doi.org/10.1029/2019ms001836, 2019.

Roach, L. A., Dörr, J., Holmes, C. R., Massonnet, F., Blockley, E. W., Notz, D., Rackow, T., Raphael, M. N., O'Farrell, S. P., Bailey, D. A., and Bitz, C. M.: Antarctic Sea Ice Area in CMIP6, Geophys. Res. Lett., 47, https://doi.org/10.1029/2019gl086729, 2020.

Roach, L. A., Eisenman, I., Wagner, T. J. W., Blanchard-Wrigglesworth, E., and Bitz, C. M.: Asymmetry in the seasonal cycle of Antarctic sea ice driven by insolation, Nat. Geosci., 15, 277–281, https://doi.org/10.1038/s41561-022-00913-6, 2022.

Saenz, B. T. and Arrigo, K. R.: Annual primary production in Antarctic sea ice during 2005–2006 from a sea ice state estimate, J. Geophys. Res.-Oceans, 119, 3645–3678, https://doi.org/10.1002/2013jc009677, 2014.

Saiki, R. and Mitsudera, H.: A Mechanism of Ice-Band Pattern Formation Caused by Resonant Interaction between Sea Ice and Internal Waves: A Theory, J. Phys. Oceanogr., 46, 583–600, https://doi.org/10.1175/jpo-d-14-0162.1, 2016.

Saiki, R., Mitsudera, H., Fujisaki-Manome, A., Kimura, N., Ukita, J., Toyota, T., and Nakamura, T.: Mechanism of ice-band pattern formation caused by resonant interaction between sea ice and internal waves in a continuously stratified ocean, Progr. Oceanogr., 190, https://doi.org/10.1016/j.pocean.2020.102474, 2021.

Screen, J. A. and Simmonds, I.: The central role of diminishing sea ice in recent Arctic temperature amplification, Nature, 464, 1334–1337, https://doi.org/10.1038/nature09051, 2010.

Simmonds, I., Keay, K., and Lim, E.-P.: Synoptic Activity in the Seas around Antarctica, Mon. Weather Rev., 131, 272–288, https://doi.org/10.1175/1520-0493(2003)131<0272:Saitsa>2.0.Co;2, 2003.

Skene, D. M., Bennetts, L. G., Meylan, M. H., and Toffoli, A.: Modelling water wave overwash of a thin floating plate, J. Fluid Mech., 777, https://doi.org/10.1017/jfm.2015.378, 2015.

Smith, D. M., Dunstone, N. J., Scaife, A. A., Fiedler, E. K., Copsey, D., and Hardiman, S. C.: Atmospheric Response to Arctic and Antarctic Sea Ice: The Importance of Ocean–Atmosphere Coupling and the Background State, J. Climate, 30, 4547–4565, https://doi.org/10.1175/jcli-d-16-0564.1, 2017.

Sørensen, H. L., Thamdrup, B., Jeppesen, E., Rysgaard, S., and Glud, R. N.: Nutrient availability limits biological production in Arctic sea ice melt ponds, Polar Biol., 40, 1593–1606, https://doi.org/10.1007/s00300-017-2082-7, 2017.

Squire, V. A.: Of ocean waves and sea-ice revisited, Cold Reg. Sci. Technol., 49, 110–133, https://doi.org/10.1016/j.coldregions.2007.04.007, 2007.

Squire, V. A.: Ocean Wave Interactions with Sea Ice: A Reappraisal, Ann. Rev. Fluid Mech., 52, 37–60, https://doi.org/10.1146/annurev-fluid-010719-060301, 2020.

Squire, V. A., Vaughan, G, L., and Bennetts, L. G.: Ocean surface wave evolvement in the Arctic Basin, Geophys. Res. Lett., 36, L22502, https://doi.org/10.1029/2009GL040676, 2009.

Stammerjohn, S., Massom, R., Rind, D., and Martinson, D.: Regions of rapid sea ice change: An interhemispheric seasonal comparison, Geophys. Res. Lett., 39, https://doi.org/10.1029/2012gl050874, 2012.

Steele, M.: Sea ice melting and floe geometry in a simple ice-ocean model, J. Geophys. Res.-Oceans, 97, 17729–17738, https://doi.org/10.1029/92jc01755, 1992.

Stopa, J. E., Sutherland, P., and Ardhuin, F.: Strong and highly variable push of ocean waves on Southern Ocean sea ice, P. Natl. Acad. Sci. USA, 115, 5861–5865, https://doi.org/10.1073/pnas.1802011115, 2018.

Sturm, M. and Massom, R. A.: Snow in the sea ice system: Friend or foe?, in: Sea Ice, edited by: Thomas, D. N., Wiley-Blackwell, Oxford, UK, 65–109, https://doi.org/10.1002/9781118778371.ch3, 2017.

Sutherland, P. and Dumont, D.: Marginal Ice Zone Thickness and Extent due to Wave Radiation Stress, J. Phys. Oceanogr., 48, 1885–1901, https://doi.org/10.1175/JPO-D-17-0167.1, 2018.

Takahashi, Y.: On the puddles of Lützow-Holm Bay, Ant. Meteorol., Pergamon Press, New York, 321–332, 1960.

Taylor, M. H., Losch, M., and Bracher, A.: On the drivers of phytoplankton blooms in the Antarctic marginal ice zone: A modeling approach, J. Geophys. Res.-Oceans, 118, 63–75, https://doi.org/10.1029/2012JC008418, 2013.

Taylor, P. D. and Feltham, D. L.: A model of melt pond evolution on sea ice, J. Geophys. Res.-Oceans, 109, https://doi.org/10.1029/2004jc002361, 2004.

Teder, N. J., Bennetts, L. G., Reid, P. A., Massom, R. A., Pitt, J. P. A., Scambos, T. A., and Fraser, A. D.: Large-scale ice shelf calving events follow prolonged amplifications in flexure, Nat. Geosci., 18, 559–606, https://doi.org/10.1038/s41561-025-01713-4, 2025.

Thomson, J. and Rogers, W. E.: Swell and sea in the emerging Arctic Ocean, Geophys. Res. Lett., 41, 3136–3140, https://doi.org/10.1002/2014gl059983, 2014.

Timco, G. W. and Weeks, W. F.: A review of the engineering properties of sea ice, Cold Reg. Sci. Technol., 60, 107–129, https://doi.org/10.1016/j.coldregions.2009.10.003, 2010.

Tison, J. L., Schwegmann, S., Dieckmann, G., Rintala, J. M., Meyer, H., Moreau, S., Vancoppenolle, M., Nomura, D., Engberg, S., Blomster, L. J., Hendricks, S., Uhlig, C., Luhtanen, A. M., de Jong, J., Janssens, J., Carnat, G., Zhou, J., and Delille, B.: Biogeochemical Impact of Snow Cover and Cyclonic Intrusions on the Winter Weddell Sea Ice Pack, J. Geophys. Res.-Oceans, 122, 9548–9571, https://doi.org/10.1002/2017jc013288, 2017.

Toffoli, A., Bennetts, L. G., Meylan, M. H., Cavaliere, C., Alberello, A., Elsnab, J., and Monty, J. P.: Sea ice floes dissipate the energy of steep ocean waves, Geophys. Res. Lett., 42, 8547–8554, https://doi.org/10.1002/2015GL065937, 2015.

Toyota, T., Takatsuji, S., and Nakayama, M.: Characteristics of sea ice floe size distribution in the seasonal ice zone, Geophys. Res. Lett., 33, https://doi.org/10.1029/2005gl024556, 2006.

Trevena, A. J. and Jones, G. B.: Dimethylsulphide and dimethylsulphoniopropionate in Antarctic sea ice and their release during sea ice melting, Mar. Chem., 98, 210–222, https://doi.org/10.1016/j.marchem.2005.09.005, 2006.

Tsamados, M., Feltham, D., Petty, A., Schroeder, D., and Flocco, D.: Processes controlling surface, bottom and lateral melt of Arctic sea ice in a state of the art sea ice model, Philos. T. R. Soc. A, 373, https://doi.org/10.1098/rsta.2014.0167, 2015.

Tschudi, M. A., Maslanik, J. A., and Perovich, D. K.: Derivation of melt pond coverage on Arctic sea ice using MODIS observations, Remote Sens. Environ., 112, 2605–2614, https://doi.org/10.1016/j.rse.2007.12.009, 2008.

Turner, J. and Comiso, J.: Solve Antarctica's sea-ice puzzle, Nature, 547, 275–277, https://doi.org/10.1038/547275a, 2017.

Uotila, P., Vihma, T., Pezza, A. B., Simmonds, I., Keay, K., and Lynch, A. H.: Relationships between Antarctic cyclones and surface conditions as derived from high-resolution numerical weather prediction data, J. Geophys. Res., 116, https://doi.org/10.1029/2010jd015358, 2011.

Urabe, N. and Inoue, M.: Mechanical Properties of Antarctic Sea Ice, J. Offshore Mech. Arct. Eng., 110, 403–408, https://doi.org/10.1115/1.3257079, 1988.

van Loon, H.: The Half-Yearly Oscillations in Middle and High Southern Latitudes and the Coreless Winter, J. Atmos. Sc., 24, 472–486, https://doi.org/10.1175/1520-0469(1967)024<0472:Thyoim>2.0.Co;2, 1967.

Vancoppenolle, M., Bopp, L., Madec, G., Dunne, J., Ilyina, T., Halloran, P. R., and Steiner, N.: Future Arctic Ocean primary productivity from CMIP5 simulations: Uncertain outcome, but consistent mechanisms, Global Biogeochem. Cy., 27, 605–619, https://doi.org/10.1002/gbc.20055, 2013.

Vichi, M., Eayrs, C., Alberello, A., Bekker, A., Bennetts, L., Holland, D., de Jong, E., Joubert, W., MacHutchon, K., Messori, G., Mojica, J. F., Onorato, M., Saunders, C., Skatulla, S., and Toffoli, A.: Effects of an Explosive Polar Cyclone Crossing the Antarctic Marginal Ice Zone, Geophys. Res. Lett., 46, 5948–5958, https://doi.org/10.1029/2019gl082457, 2019.

Vihma, T., Johansson, M. M., and Launiainen, J.: Radiative and turbulent surface heat fluxes over sea ice in the western Weddell Sea in early summer, J. Geophys. Res.-Oceans, 114, https://doi.org/10.1029/2008jc004995, 2009.

Wadhams, P.: The Seasonal Ice Zone. In: The Geophysics of Sea Ice, edited by: Untersteiner, N., Springer, Boston, USA, 825–991, https://doi.org/10.1007/978-1-4899-5352-0_15, 1986.

Wadhams, P.: Ice In The Ocean, CRC Press, UK, 364 pp, ISBN 9789056992965, 2000.

Wadhams, P., Lange, M. A., and Ackley, S. F.: The ice thickness distribution across the Atlantic sector of the Antarctic Ocean in midwinter, J. Geophys. Res.-Oceans, 92, 14535–14552, https://doi.org/10.1029/JC092iC13p14535, 1987.

Wang, Q., Li, Z., Lu, P., Xu, Y., and Li, Z.: Flexural and compressive strength of the landfast sea ice in the Prydz Bay, East Antarctic, The Cryosphere, 16, 1941–1961, https://doi.org/10.5194/tc-16-1941-2022, 2022.

Wang, S., Maltrud, M., Elliott, S., Cameron-Smith, P., and Jonko, A.: Influence of dimethyl sulfide on the carbon cycle and biological production, Biogeochemistry, 138, 49–68, https://doi.org/10.1007/s10533-018-0430-5, 2018.

Warren, S. G.: Optical properties of snow, Rev. Geophys. Space Phys., 20, 67–89, https://doi.org/10.1029/RG020i001p00067, 1982.

Warren, S. G.: Optical properties of ice and snow, Philos. T. R. Soc. A., 377, 20180161, https://doi.org/10.1098/rsta.2018.0161, 2019.

Warren, S. G., Hahn, C. J., London, J., Chervin, R. M., and Jenne, R. L.: Global distribution of total cloud cover and cloud type amounts over the ocean, USDOE Office of Energy Research, Washington, DC (USA). Carbon Dioxide Research Div.; National Center for Atmospheric Research, Boulder (USA), https://doi.org/10.5065/D6QC01D1, 1988.

Webster, M., Gerland, S., Holland, M., Hunke, E., Kwok, R., Lecomte, O., Massom, R., Perovich, D., and Sturm, M.: Snow in the changing sea-ice systems, Nat. Clim. Change, 8, 946–953, https://doi.org/10.1038/s41558-018-0286-7, 2018.

Webster, M. A., Holland, M., Wright, N. C., Hendricks, S., Hutter, N., Itkin, P., Light, B., Linhardt, F., Perovich, D. K., Raphael, I. A., Smith, M. M., von Albedyll, L., and Zhang, J.: Spatiotemporal evolution of melt ponds on Arctic sea ice, Elem. Sc. Anthrop., 10, https://doi.org/10.1525/elementa.2021.000072, 2022.

Williams, R. G., Ceppi, P., Roussenov, V., Katavouta, A., and Meijers, A. J. S.: The role of the Southern Ocean in the global climate response to carbon emissions, Philos. T. R. Soc. A, 381, 20220062, https://doi.org/10.1098/rsta.2022.0062, 2023.

Williams, T. D., Bennetts, L. G., Squire, V. A., Dumont, D., and Bertino, L.: Wave–ice interactions in the marginal ice zone. Part 1: Theoretical foundations, Ocean Model., 71, 81–91, https://doi.org/10.1016/j.ocemod.2013.05.010, 2013.

Worby, A. P., Massom, R. A., Allison, I., Lytle, V. I., and Heil, P.: East Antarctic Sea Ice: A Review of Its Structure, Properties and Drift. In: Antarctic Sea Ice: Physical Processes, Interactions and Variability, edited by: Jeffries, M. O., Antarctic Research Series, American Geophysical Union, Washington DC, USA, 41–67, https://doi.org/10.1029/AR074p0041, 1998.

Young, I. R. and Ribal, A.: Multiplatform evaluation of global trends in wind speed and wave height, Science, 364, 548–552, https://doi.org/10.1126/science.aav9527, 2019.

Young, I. R., Fontaine, E., Liu, Q., and Babanin, A. V.: The Wave Climate of the Southern Ocean, J. Phys. Oceanogr., 50, 1417–1433, https://doi.org/10.1175/jpo-d-20-0031.1, 2020.

Zatko, M. C. and Warren, S. G.: East Antarctic sea ice in spring: spectral albedo of snow, nilas, frost flowers and slush, and light-absorbing impurities in snow, Ann. Glaciol., 56, 53–64, https://doi.org/10.3189/2015AoG69A574, 2015.

Zeebe, R. E., Eicken, H., Robinson, D. H., Wolf-Gladrow, D., and Dieckmann, G. S.: Modeling the heating and melting of sea ice through light absorption by microalgae, J. Geophys. Res.-Oceans, 101, 1163–1181, https://doi.org/10.1029/95jc02687, 1996.